

LAPPEENRANTA UNIVERSITY OF TECHNOLOGY
LUT School of Energy Systems
Energy Technology

Alla Toktarova

**LONG-TERM LOAD FORECASTING IN HIGH RESOLUTION FOR ALL
COUNTRIES GLOBALLY**

Examiner: Professor Christian Breyer, LUT
Professor Esa Vakkilainen, LUT
Supervisor: Professor Christian Breyer, LUT

ABSTRACT

Lappeenranta University of Technology
LUT School of Energy Systems
Energy Technology

Alla Toktarova

Long-term load forecasting in high resolution for all countries globally

Master's thesis

2017

59 pages, 26 figures, 2 tables and 5 appendices

Examiners: Professor Christian Breyer
Professor Esa Vakkilainen

Keywords: electricity demand, load curve, modelling, long-term load forecasting,

Electricity demand modelling is the central and integral issue for the planning and operation of electric utilities, energy suppliers, system operators and other market participants. Load forecasting provides important information for electricity network planning, and it is essential for the electricity system development. The increase of interest in these issues has occurred as a result of liberalization of power markets, the aging infrastructure and high penetration rate of renewables.

In this research, a methodology is proposed for modelling and forecasting electricity demand. The major advantage of the proposed approach is that it enables the possibility of making short-and long-term hourly load forecasting within a single framework for all countries. The method is constructed and verified using 56-real load data of diverse countries. The accuracy of proposed model function is represented in terms of R-squared error.

The model estimates the amplitude of demand fluctuations for certain significant frequencies and generates the total hourly demand curve for a given year, based on a superposition of sine functions. The initial step was to construct the database including socio-economic and meteorological data for all countries. The world socio-economic scenario is projected from historical values using logistic growth functions. Based on this socio-economic scenario, the annual total demand and peak demand were obtained for all countries, for a period from 2017 to

2100. Finally, the sum of various sine functions can be used to calibrate and forecast hourly electricity demand for any country with available input data for any year in the addressed period.

A key result found is that specific economic, technical and climate characteristics, such as high shares of marginal cost generation, air conditioning, impact of tourism and industrial consumption, local temperature and seasonal effects have significant influence on the quality of results. The obtained results could have a significant impact and support in energy transition studies towards sustainability.

ACKNOWLEDGMENTS

Nothing impossible. I will forever grateful to Lappeenranta University of Technology for “open mind”.

I would like to thank my supervisor, Professor Christian Breyer, for the opening to me a renewable energy based world, for this risky and interesting topic and for all his countless support on this time in LUT. I extend my deepest thanks to the supervisors of this work, Professor Christian Breyer and Professor Esa Vakkilainen for their guidance and valuable contribution to the work.

It was pleasure work in Solar Economy group. I'd like to thank my international, colorful, solar family in particular Narges, Upeksha, Arman, Mahdi, Ashish, Marzella, Olya, Larissa, Javier, Solomon S., Maulidi, Abdelrahman, Anil, Manish, Siavash, Dominik, Svetlana, Alexander, Kristina, Michael, Solomon A., Dmitriy, Alena, Eetu, Otto for the lovely time being. Individual thanks to Upeksha Caldera for her valuable comments and revision of the language in the preparation of this thesis. However, I am solely responsible for any remaining errors.

Special thanks to my Lappeenranta gang: Iullia Shnai, Elizaveta Drobysheva, Eugenia Vanadzina, Gera Minkin, Andrey Ivanov, Toivo Toikka. You take place in my soul. Stay swag, fight or die and always remember take fotos. Thank you Kendrick Lamar for “DAMN.” and Lana Del Rey for “Lust for Life”. Words can't describe how thankful I am to Jack Little, Cleve Moler and Steve Bangert for The MathWorks and for Matlab in particular.

Finally, my warmest thanks go to my family, relatives, Ksenia Vinogradova, Olga Vartanova and Ulyana Kurilo. They have spurred me all my life.

Alla Toktarova

Lappeenranta 10.08.2017

CONTENTS

1. INTRODUCTION	8
2. DATA	10
2.1 Available load data	10
2.2 Economic Data.....	10
2.3 Annual Electricity Demand and Peak Load	11
2.4 Temperature	13
2.5 Electricity Production, Industrial Power Consumption, Contribution Tourism to GDP.....	14
3. METHODOLOGY	15
3.1 Annual consumption trend.....	15
3.2 Annual oscillation	15
3.2.1 Basic annual oscillation	16
3.2.2 Annual oscillation driven by electric heating.....	18
3.3 Diurnal oscillation.....	19
3.3.1 Basic diurnal oscillation.....	19
3.3.2 Diurnal oscillation driven by low electricity prices	21
3.3.3 Double frequency of diurnal oscillation.....	21
3.4 Optimal summer day oscillation	22
3.5 Week oscillation.....	22
3.5.1 Basic week oscillation.....	22
3.5.2 Double frequency of week oscillation.....	24
3.6 Weekend oscillation.....	24
3.6.1 Basic weekend oscillation.....	24
3.6.2 Double frequency of weekend oscillation.....	25
3.6.3 Decreased weekend average	25
3.7 Afternoon and evening peak	26
3.8 Air conditioning	27
3.8.1 Day peak	27
3.8.2 Summer night peak	28
3.8.3 Winter peak	29
3.9 Travel and tourism contribution.....	30
3.10 Maximum demand consumption.....	31
3.11 Calibration total annual demand	32
3.12 Estimation of future electricity demand and load profile.....	32

4. RESULTS AND APPLICATION	33
4.1 Modeled load curve quality.....	33
4.2 Modeled peak load quality.....	34
4.3 Model results for exemplarily countries and special impact variables	35
4.3.1 Impact variables	35
4.3.2 Sweden.....	39
4.3.3 Iran	43
4.4 Forecast of electricity demand and the respective load profile.....	47
5. DISCUSSION	50
6. CONCLUSION	53
7. REFERENCES	54
8. APPENDIX	62

NOMENCLATURE

a^j		Amplitude
b^j		Frequency
c^j		Phase of shift
d^j		Additional ordinate offset
d_{first}		First day of year (from Monday to Sunday, 1-7)
E^{tj}_{ave}	[MW]	Average electricity consumption over the year
E^{tj}_{cap}	[kWh/cap]	Electricity consumption per capita
E^{j}_{hmg}	[%]	Proportion of the electricity generation share of hydro, nuclear and geothermal power plants in a country j
E^{j}_{ind}	[%]	Industry factor, i.e. the power consumption in the industrial sector
E^{tj}_y	[TWh]	Annual electricity consumption
GDP^{tj}_{cap}	[€/cap]	Gross Domestic Product per capita
GDP^{j}_{To}	[%]	Tourism and travel share in GDP
n^j		Extent of sine
Lat^j	[°]	Latitude
Lon^j	[°]	Longitude
$Peak^{tj}$	[MW]	Maximum electricity demand for the years 2017-2100
$Sunset$	[h]	Vector with the time of sunset for the specific geographical region
$T^{j}_{c\ month}$	[°C]	Average temperature of the coldest month
$T^{j}_{local\ hours}$	[°C]	Vector of temperature for each hour of year for “nearest” point to the geographical location
T^{j}_w	[°C]	Warmest Temperature
$T^{j}_w\ month$	[°C]	Average temperature of the warmest month
ΔT^j	[°C]	Difference of the warmest and the coldest month temperature
i		Number of sine function
j		Country index
t		Year index

1. INTRODUCTION

Electricity demand modelling and forecasting are vital issues in effective operation and planning of power systems. The liberalization of power markets, the aging infrastructure and high penetration rate of renewables have further increased interest for electricity consumption forecasting [1].

Depending on the time horizon and the operating decisions that needs to be made electric load forecasts are categorized as short-term, medium-term and long-term [2]. Long-term demand forecasting indicating the prediction horizon from several months to several years ahead is an important component in planning new electricity facilities and development of transmission and distribution systems [3]. Short-term forecasting is needed for the operation of today's power systems [4]. In current research on load, short-term demand forecasting prevails and attracts more attention than long-term demand forecasting [3, 5]. A large variety of methods and ideas has been tried for load forecasting, with varying degrees of success. In the following, a short overview over some of the models and methods is given.

Table 1. Overview of forecasting methods and related resources.

Methods	Sources
1. Statistical methods	
Regression-based models	[3], [6-13]
Time-series approaches	[14-15],
Exponential smoothing	[16]
2. Artificial intelligence based methods	
Artificial neural networks	[10], [17-18]
Fuzzy logic	[19-22]
Support vector machines	[23]

Regression, as a statistical model, is a widely used technique for electric load forecasting [1]. The load is represented as a function of some descriptor variables [24]. The explanatory variables and their functional forms are key concepts for accuracy and precision of a forecast [17].

Bianco et al. [8] suggested a linear regression model for forecasting long-term annual electricity consumption in Italy, based on GDP and population, up to 2030. Mohamed et al. [9] built a multiple linear regression model to predict electricity consumption for New Zealand, thoroughly

investigating the effects of GDP, population and price of electricity on annual load. Hor et al. [7] studied the influence of weather variables and socio-economic factors on the monthly electricity demand in England and Wales by using multiple regression analysis. Kankal et al. [10] expressed energy consumption patterns for Turkey as functions of socio-economic and demographic variables using regression analysis and artificial networks. Günay [17] also used multiple linear regression and artificial networks approaches to describe the demand as a function of population, gross domestic product per capita, inflation percentage, unemployment percentage and average temperature to forecast annual electricity demand. The results were presented for Turkey until the year 2028 with an annual resolution. Hong et al. [6] proposed a probabilistic forecasting approach modernized with hourly demand data and multiple linear regression for long-term electricity forecasting. The proposed approach has been deployed across many U.S. utilities.

Similarly, in the majority of presented studies, the period of forecast is relatively short and the described electricity load pattern has a low resolution. Recently, there has been a trend towards modeling and long-term forecasting electricity consumption in high resolution [2]. Trotter et al. [12] proposed a method to forecast the Brazilian electricity demand for the period 2016 to 2100 paying particular attention to weather uncertainty. Another specific of all studies is the focus on only one particular country [8-10, 17,25-26]. Yukseltan et al. [11] suggested to apply their model to any country but quantitative results were presented only for Turkey.

In this paper, a methodology to model and forecast electricity demand on a national level with an hourly time scale for every year, between 2016 and 2100, is proposed. The remaining parts of the paper are organized as follows. Section 2 describes the data and variables construction. In section 3 we present linear regression model using the sum of various sine functions to calibrate and forecast electricity demand. Applications of the model and forecasting accuracy results are presented in section 4. In section 5 the main contributions of this paper are highlighted and possible research directions are discussed. Section 6 draws the conclusions.

2. DATA

Determination of the relevant variables affecting electricity demand and selecting the appropriate model basis is an important step in modelling and forecasting electricity demand. The applied parameters are well known and most commonly used in the literature [27], such as existing load data, economic data, annual electricity consumption, annual peak load, temperature and some country-specific economic data.

2.1 Available load data

The set of countries with available real electric load data and real peak data is presented in the Appendix (Table A1). The collected data has been used to calibrate and verify the synthetic load model. Figure 1 illustrates the collected data and how representative the different regions in the world are represented by load data in full hourly resolution for an entire year, or at least by the peak load.

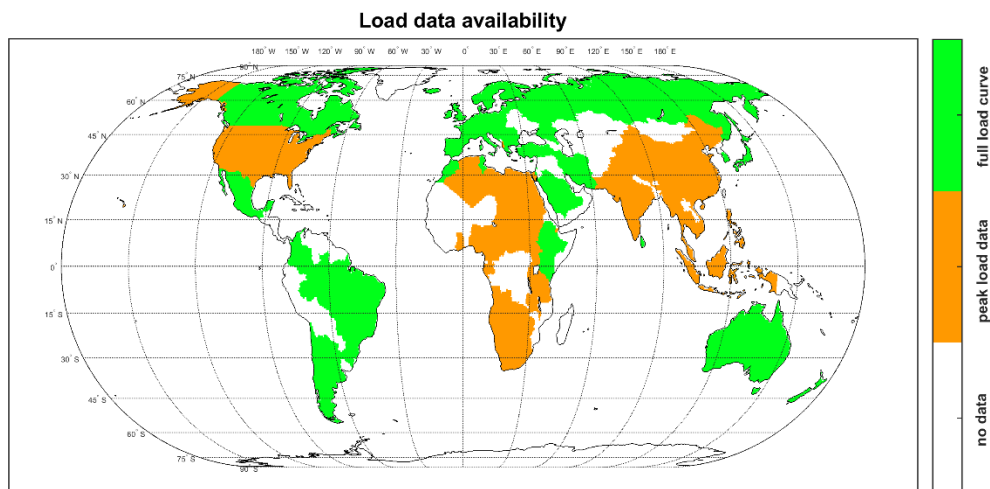


Fig. 1. Available load data in full hourly resolution for an entire year (green) and peak load data (orange).

2.2 Economic Data

A strong relationship between electricity consumption and economic growth could have been confirmed [28-30]. In this paper, the gross domestic product (GDP) per capita in purchasing power parity (PPP) data has been chosen as economic indicator. The World Bank and IEA provide GDP

per capita values worldwide for the period 1990-2014 [31]. Long term GDP per capita forecast was modelled by applying a logistic-growth function [32] based on the assumption that by the year 2100 goals set in the UN Resolution adopted by the General Assembly will be achieved and inequalities between countries will be declined [33]. Eq (1) is the logistic growth function in its generalized form.

$$f(t) = A + \frac{K-A}{1+10^{-B(t-M)}} \quad (1)$$

where t is time, A is lower asymptote, K is upper asymptote, B is growth rate and M is time of maximum growth.

The population weighted average value of GDP per capita of the 30 countries with highest GDP per capita in the period from 1990 to 2014 has been adopted as a reference line of convergence for all countries in the year 2100, assuming that GDP per capita's growth rate in the leading countries will be equal to the rate of growth over the past 25 years, which had been 1.0% per year in real terms. This long-term stable economic growth of the reference wealth level leads to a global unique GDP per capita of 88000 € in the year 2100. The long-term exchange rate of 1.33 USD/€ is employed.

2.3 Annual Electricity Demand and Peak Load

Historical data on annual electricity demand per country is provided by IEA [34-35]. Based on the assumption that electricity consumption is closely associated with the national economy [36], the world global electricity demand trend was found as a function of GDP per capita by a two-term exponential function. Electricity per capita values were found by applying population data developed by the UN Department of Economic and Social Affairs [37].

Correlation between electricity per capita and GDP per capita values for the year 2012 are visualized in Figure 2. Wealthy countries have a stronger correlation between electricity demand and the value of GDP per capita than poor countries. It is also found that the energy intensity decreases for higher GDP, since the energy intensity per additional GDP shows a negative gradient (Figure 2 right).

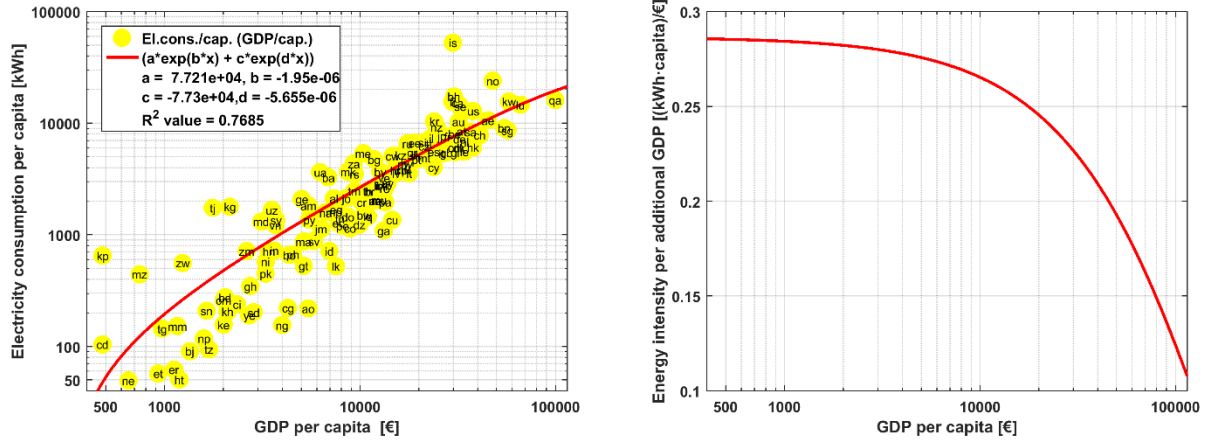


Fig. 2. Electricity consumption per capita as a function of GDP per capita for the year 2012 (left) and the derivation of the smoothing function (right).

The Eq. (2) represents the dependence of electricity consumption per capita (E_{cap}^{tj}) on GDP per capita (GDP_{cap}^{tj}) for a certain country j and year t .

$$E_{cap}^{tj} = a \cdot e^{(b \cdot GDP_{cap}^{tj})} + c \cdot e^{(d \cdot GDP_{cap}^{tj})} \quad (2)$$

Coefficients are:

$$a = 7.721 \cdot 10^4 \text{ kWh}, \quad b = -1.95 \cdot 10^{-6} \text{ 1}/(\text{€}/\text{capita}), \quad c = -7.73 \cdot 10^4 \text{ kWh}, \quad d = -5.655 \cdot 10^{-6} \text{ 1}/(\text{€}/\text{capita}).$$

The Eq. (2) is used for estimating the electricity consumption per capita for the years 2013 to 2100. This equation describes global electricity demand trend. In the model weighted average electricity demand values are used as future trend. The trend was formed by the convergence of the individual countries electricity demand trend lines to the global demand trend. The convergence growth rate equals to 2% per year from the year 2013. Starting from the year 2060 countries electricity demand has been calculated according to global trend presented in Eq. (2).

The dependence of peak demand per capita on GDP per capita has been established using the linear regression method. The correlation between peak demand per capita and GDP per capita for country j and year t is shown in the Figure 3.

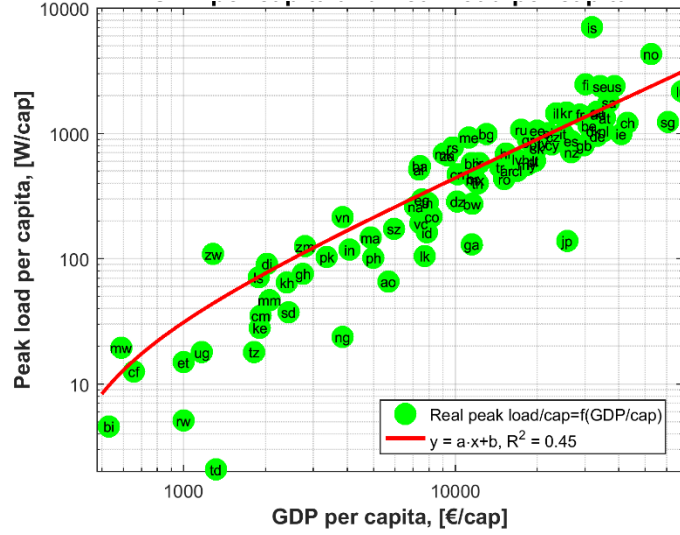


Fig. 3. Peak demand per capita as a function of GDP per capita.

The future projection of peak demand per capita is calculated based on the Eq. (3).

$$Peak^{tj} = a \cdot GDP^{tj}_{cap} + b \quad (3)$$

where a is 0.0456 W/€ and b is 14.48 W/capita.

The synthetic values of peak demand taking into account the deviation from the individual peak demand of country in reference to the trend line in percent are used as input variable in the model for countries with available peak demand data maintaining the relative individual peak from the trend line. For countries with unknown peak demand data the global synthetic peak demand trend line is used.

2.4 Temperature

Mirasgedis et al. [13] illustrated the influence of the temperature on electricity consumption. In this research, the data of hourly temperature from 1984 to 2005 is obtained from NASA databases [38-39] and partly reprocessed by the German Aerospace Center [40]. The global temperature raw data are stored in Kelvin units gridded in $0.45^0 \times 0.45^0$ degree on an hourly basis. For the further calculation, these data are converted in °C and aggregated on a daily and monthly basis. In the model it will be used in hourly resolution as well as in daily and monthly aggregation.

2.5 Electricity Production, Industrial Power Consumption, Contribution Tourism to GDP

The ratio of industrial electricity consumption to total electricity consumption is taken from [34-35] and defines the industrialisation of a region. If this value is not available, the corresponding ratio of industrial GDP to total GDP from [43] is used. The higher the level of industrialisation the stronger the baseload characteristic of the entire load curve and the lower is the ratio of minimum to maximum load.

To take into account the impact of baseload power sources with low marginal costs the ratio of electricity sourced from hydro, nuclear and geothermal power to total generated electricity [34-35] is used in the model. This has an impact in the northern hemisphere on electricity-based heating.

The contribution of travel and tourism to GDP [42] is used in the model in order to take into account peak loads during the tourist season. Such an impact can be observed for classical tourist countries, which are quite often islands in sunny regions.

3. METHODOLOGY

Load patterns depend on the month of year, day of the week, and hour of a day [1]. The real load profiles (see Table A1) show multilevel seasonality governed by periodical astronomical events affecting temperature, lighting and climate at a given location, but also regular cultural and economic characteristics. As the main model-building approach, the sum of sine functions was chosen to describe various relationships between demand and underlying influencing parameters. The model is represented by the following fundamental equations (4) describing the load:

$$load(x) = \sum_i y_i(x) = \sum_i a_i \sin^{n_i} (b_i x + c_i) + d_i \quad (4)$$

Where x is the time in hours since the beginning of the year, running from 1 to 8760. Additional parameters are a_i the amplitude, b_i the frequency, c_i the phase shift, d_i the additional ordinate offset, n_i the power of sine (only values 1 and 2 are used) and i denotes the number of sine functions used to describe the full load curve.

3.1 Annual consumption trend

The average consumption in MW is set to the arithmetic mean of the annual electricity consumption expressed in TWh equally distributed to all hours of the year. The average consumption ensures a constant bias of electricity consumption for all hours of the year.

$$y_1 = a_1 \sin^{n_1} (b_1 x + c_1) + d_1 \quad (5)$$

$$a_1 = 0 \quad (5a) \quad b_1 = 0 \quad (5b) \quad c_1 = 0 \quad (5c) \quad n_1 = 0 \quad (5d)$$

$$d_1 = E_y^{tj} \frac{10^6}{8760 h} \quad (5e)$$

Where E_y^{tj} is the electricity consumption of the regarded year and country in TWh.

3.2 Annual oscillation

3.2.1 Basic annual oscillation

Three basic patterns have been revealed for annual oscillation: (i) Temperature has a significant fundamental influence on the annual oscillation of electricity consumption for all countries. (ii) The demand is observed to be higher on cold days. (iii) However, on hot days the demand is also increased due to air conditioning.

$$y_2 = a_2 \sin^{n_2} (b_2 x + c_2) + d_2 \quad (6)$$

$$d_2 = 0 \quad (6a) \quad n_2 = 1 \quad (6b)$$

The frequency of the annual cycle is b_2 . The number 8760 in the denominator stands for the number of observations in the period, here: hours in a year as an hourly sampled data set is used.

$$b_2 = \frac{2\pi}{8760} \quad (6c)$$

The time shift parameter c_2 differs for the northern and southern hemisphere. The latitude in the formula is defined as follows:

$$c_2 = 0.225 \cdot 2\pi \frac{lat}{|lat|} \quad (6d)$$

Countries where the difference between the warmest and the coldest monthly averaged temperature ΔT^j varies from 0 to 3.1 °C show a constant electricity demand without significant peaks during the year.

$$f_{a_2}^1(\Delta T^j) = \begin{cases} 1, & \Delta T^j < 3.1 \\ 0, & \Delta T^j \geq 3.1 \end{cases} \quad (6e)$$

$$a_2^1 = 0 \quad (6f)$$

A sharp increase of electricity consumption in summer period is observed in regions, where warmest temperature T_w^j can exceed 32.41 °C during the year.

$$f_{a_2}^2(T_{c\,month}^j) := \begin{cases} 1, & T_{c\,month}^j \geq 32.41 \\ 0, & T_{c\,month}^j < 32.41 \end{cases} \quad (6g)$$

$$f_{a_2}^3(lat^j) := \begin{cases} 1, & lat^j \in [-34, 35] \\ 0, & lat^j \in [-90, -34) \cup (35, 90] \end{cases} \quad (6h)$$

$$a_2^2 = E_{ave}^{tj} \left(1 - e^{-\frac{32.2 - T_{c\ month}^j}{47.9}} \right) \quad (6i)$$

Where E_{ave}^{tj} is average electricity consumption over the year and $T_{c\ month}^j$ is average temperature of the coldest month.

For other countries the seasonal demand pattern exhibits higher consumption during winter than in summer.

$$f_{a_2}^4(T_{c\ month}^j) := \begin{cases} 1, & T_{c\ month}^j < 32.41 \\ 0, & T_{c\ month}^j \geq 32.41 \end{cases} \quad (6j)$$

$$f_{a_2}^5(lat^j) := \begin{cases} 1, & lat^j \in [-90, -34) \cup (35, 90] \\ 0, & lat^j \in [-34, 35] \end{cases} \quad (6k)$$

$$a_2^3 = 0.1335 \cdot E_{ave}^{tj} \left(1 - e^{-\frac{12.5 - T_{c\ month}^j}{15.2}} \right) \quad (6l)$$

Where E_{ave}^{tj} is average electricity consumption over the year and $T_{c\ month}^j$ is average temperature of the coldest month.

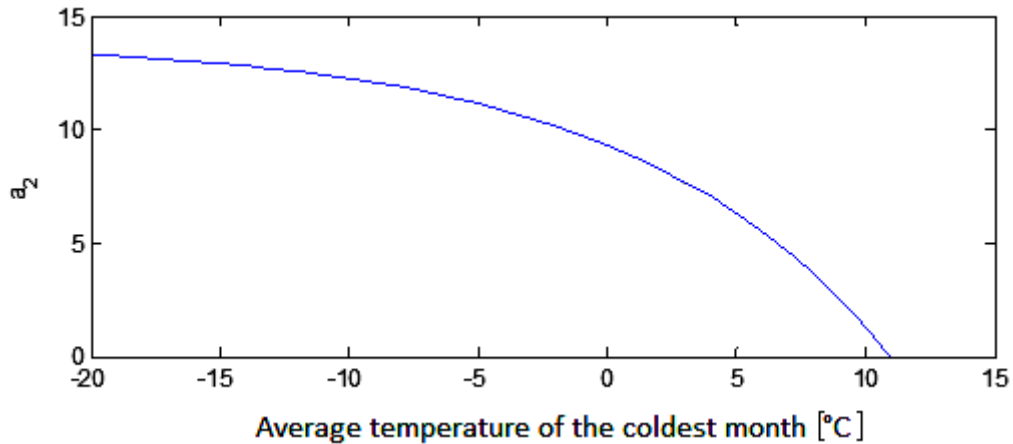


Fig. 4. Dependence of coefficient a_2 on average temperature of coldest month $T_{c\ month}^j$.

$$a_2 = a_2^1 \cdot f_{a_2}^1(\Delta T^j) + a_2^2 \cdot f_{a_2}^2(T_{c\ month}^j) \cdot f_{a_2}^3(lat^j) + a_2^3 \cdot f_{a_2}^4(T_{c\ month}^j) \cdot f_{a_2}^5(lat^j) \quad (6m)$$

3.2.2 Annual oscillation driven by electric heating

The effect of increased electricity demand on cold days is substantially higher, than on average of the countries, in case of a high proportion of hydro, nuclear and geothermal generation of electricity in the total annual production. Such generation is characterised by rather low marginal cost, which leads to use electric heating to meet heat demand during the cold season.

$$y_3 = a_3 \sin^{n_3} (b_3 x + c_3) + d_3 \quad (1)$$

$$d_3 = 0 \quad (7a) \quad n_3 = 1 \quad (7b)$$

The frequency and the time shift are equal to the basic annual oscillation (6c), (6d).

$$b_3 = b_2 = \frac{2\pi}{8760} \quad (7c) \quad c_3 = c_2 = 0.225 \cdot 2\pi \frac{lat}{|lat|} \quad (2)$$

The amplitude value for annual oscillation driven by heating electricity is calculated for regions where $T_{w\ month}^j > 12$ °C, $T_{c\ month}^j < 11$ °C, $\Delta T^j > 5$ °C and E_{hng}^j varies between 80% and 100%.

$$f_{a_3}^1(T_{w\ month}^j) = \begin{cases} 1, & T_{w\ month}^j \geq 12 \\ 0, & T_{w\ month}^j < 12 \end{cases} \quad (7e)$$

$$f_{a_3}^2(T_{c\ month}^j) := \begin{cases} 1, & T_{c\ month}^j \leq 11 \\ 0, & T_{c\ month}^j > 11 \end{cases} \quad (7f)$$

$$f_{a_3}^3(\Delta T^j) = \begin{cases} 1, & \Delta T^j \geq 5 \\ 0, & \Delta T^j < 5 \end{cases} \quad (7g)$$

$$f_{a_3}^4(E_{hng}^j) := \begin{cases} 1, & E_{hng}^j \in [80, 100] \\ 0, & E_{hng}^j \in (0, 80) \end{cases} \quad (7h)$$

$$a_3^1 = \frac{(11 - T_{c\ month}^j) \cdot E_{ave}^{tj}}{100} \cdot E_{hng}^{tj} \quad (7i)$$

Where $T_{c\ month}^j$ is the average temperature of the coldest month, E_{ave}^{tj} is the average electricity consumption over the year and E_{ind}^j is the industry factor representing the power consumption in the industrial sector.

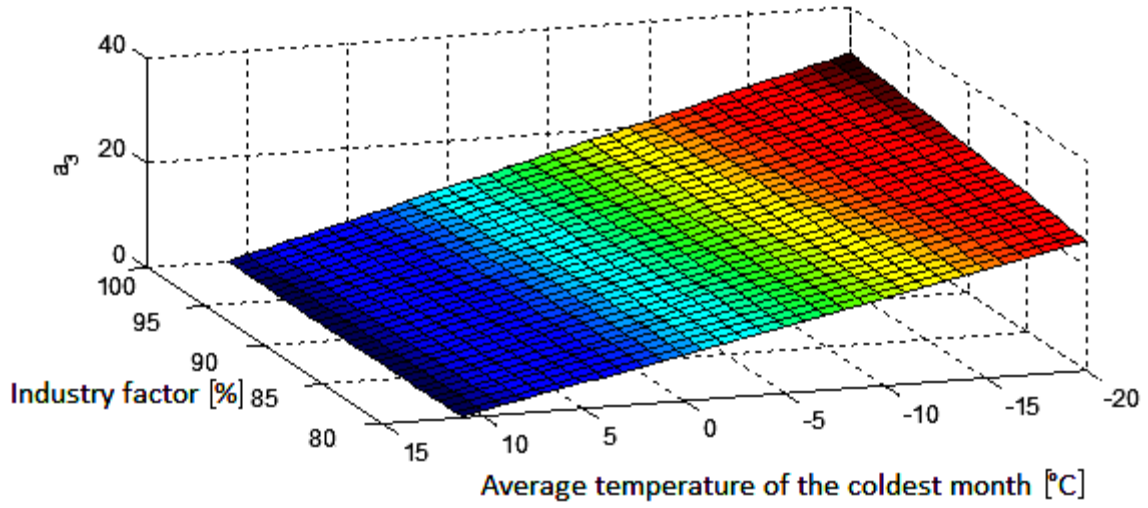


Fig. 5. Dependence of coefficient a_3 on average temperature of coldest month $T_{c\ month}^j$ and industry factor E_{ind}^j .

$$a_3 = a_3^1 \cdot f_{a_3}^1(T_w^j) \cdot f_{a_3}^2(T_c^j) \cdot f_{a_3}^3(\Delta T^j) \cdot f_{a_3}^4(E_{hng}^j) \quad (7i)$$

Where T_w^j is the average temperature of the warmest month, T_c^j is the average temperature of the coldest month, ΔT^j is the temperature difference of the warmest and the coldest month and E_{hng}^j is the proportion of the electricity generation share of hydro, nuclear and geothermal power plants.

3.3 Diurnal oscillation

3.3.1 Basic diurnal oscillation

The electricity consumption pattern over a day shows substantial intraday variability. The demand is higher than average during noon and evening, while night demand tends to be lower than average.

$$y_4 = a_4 \sin^{n_4}(b_4 x + c_4) + d_4 \quad (8)$$

$$d_4 = 0 \quad (8a) \quad n_4 = 1 \quad (8b)$$

Periods of 24 and 12 hours are introduced to model daily oscillations.

$$b_4 = \frac{2\pi}{8760} \cdot 365 \quad (8c)$$

One hour corresponds to $2\pi/24$. The minimum point is $2/3\pi$, this corresponds to 18 o'clock. It is assumed that the lowest demand during the day corresponds to 3 o'clock in the morning. This implies a phase shift of 9 hours, which had been fine tuned to 9.1 hours, as realised by the parameter c_4 .

$$c_4 = -9.1 \frac{2\pi}{24} \quad (8d)$$

The magnitude of the amplitude follows a decreasing exponential function.

$$a_4 = 0.12 \cdot E_{ave}^{tj} \cdot \left(1 - e^{-\frac{-GDP_{cap}^{tj}}{10}} \right) \quad (8e)$$

Where E_{ave}^{tj} is average electricity consumption over the year and GDP_{cap}^{tj} is the gross domestic product per capita.

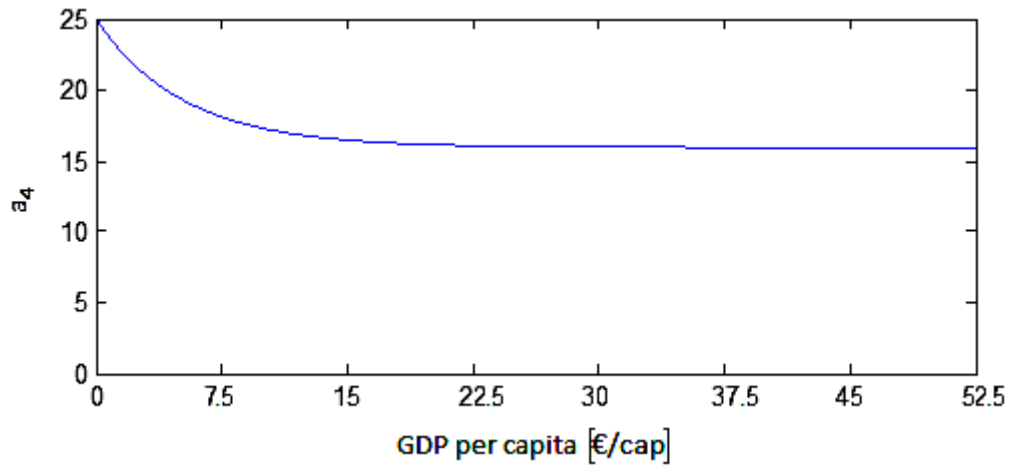


Fig. 6. Dependence of coefficient a_4 on GDP per capita, GDP_{cap}^{tj}

3.3.2 Diurnal oscillation driven by low electricity prices

A high national share of hydropower, geothermal or nuclear energy typically implies low energy prices, which in turn lead to in general more electricity consumption due to a lower level of efficiency.

$$y_5 = a_5 \sin^{n_5} (b_5 x + c_5) + d_5 \quad (9)$$

$$d_5 = 0 \quad (9a) \quad n_5 = 1 \quad (9b)$$

The frequency is equal to the basic diurnal oscillation (8c).

$$b_5 = b_4 = \frac{2\pi}{8760} \cdot 365 \quad (9c)$$

Sine, shifted by π , oscillation reduces the amplitude of the basic diurnal oscillation.

$$c_5 = c_4 + \pi = 2.9 \frac{2\pi}{24} \quad (9d)$$

Amplitude for daily oscillations is driven by low electricity prices induced by a high share of low marginal cost generation, which is indicated by the supply share of hydropower, nuclear and geothermal energy ($E^{j_{hng}}$) and applied for a respective share of higher than 80% in the total electricity supply. The function Eq. (7h) described above in the section 3.2.2 is used to define amplitude of diurnal oscillation driven by low electricity prices.

$$a_5^1 = 0.12 \cdot E_{ave}^{tj} \cdot (E_{hng}^{tj})^8 \quad (9e)$$

$$a_5 = a_5^1 \cdot f_{a_3}^4(E_{hng}^j) \quad (9f)$$

Where E_{ave}^{tj} is average electricity consumption over the year.

3.3.3 Double frequency of diurnal oscillation

The available load data exhibit a double peak structure, i.e. one peak around noon and another in the later afternoon to early evening.

$$y_6 = a_6 \sin^{n_6} (b_6 x + c_6) + d_6 \quad (10)$$

$$d_6 = 0 \quad (10a) \quad n_6 = 1 \quad (10b)$$

The period 12 hours is introduced to simulate a daily double peak oscillation.

$$b_6 = \frac{2\pi}{8760} \cdot 365 \cdot 2 \quad (10c)$$

$$c_6 = 2 \cdot c_4 - \frac{3}{2}\pi = -36.2 \frac{2\pi}{24} \quad (10d)$$

$$a_6 = \frac{(a_4 - a_5)}{2.71} = 0.044 \cdot E_{ave}^{tj} \left(\left(1 - e^{-\frac{-GDP_{cap}^{tj}}{10}} \right) - (E_{hng}^{tj})^8 \cdot f_{a_3}^4 (E_{hng}^j) \right) \quad (10e)$$

3.4 Optimal summer day oscillation

This oscillation is almost identical to the double peak structure of Eq. (10), however the phase shift is chosen so that the afternoon peak disappears and the amplitude is weaker.

$$y_7 = a_7 \sin^{n_7} (b_7 x + c_7) + d_7 \quad (11)$$

$$d_7 = 0 \quad (11a) \quad n_7 = 1 \quad (11b)$$

$$b_7 = b_6 = \frac{2\pi}{8760} \cdot 365 \cdot 2 \quad (11c)$$

$$c_7 = -2 \cdot c_6 + \pi = 84.4 \frac{2\pi}{24} \quad (11d)$$

$$a_7 = \frac{a_4}{3.7} = 0.032 \cdot E_{ave}^{tj} \cdot \left(1 - e^{-\frac{-GDP_{cap}^{tj}}{10}} \right) \quad (11e)$$

3.5 Week oscillation

3.5.1 Basic week oscillation

Electricity demand is not uniform throughout the week. It peaks during weekdays' working hours and is at its minimum during nights and weekends.

$$y_8 = a_8 \sin^{n_8} (b_8 x + c_8) + d_8 \quad (12)$$

$$d_8 = 0 \quad (12a) \quad n_8 = 1 \quad (12b)$$

Frequency of a weekly cycle expressed in hourly terms:

$$b_8 = \frac{2\pi}{8760} \cdot \frac{365}{7} \quad (12c)$$

It is assumed that the lowest electricity demand of the weekly oscillation equals 3 o'clock of Sunday morning. This hour conforms the 147th hour of a week. For a given a length of the period of 168 hours (24 h·7 = 168 h), the lowest load of the week is equal to 126th hour of the week (168·3/2·π, since 3/2·π equals the minimum of the sine function). The phase shift is therefore (126-147)/168·2π = -0.25π. The phase shift follows to:

$$c_8 = -0.25\pi + (d_{first} - 1) \cdot \frac{2\pi}{7} \quad (12d)$$

Where d_{first} is the first day of the year $\epsilon \mathbb{N}, [1,7]$ for Monday =1 and Sunday = 7.

Countries with the weekend on Friday and Saturday have the lowest demand of the weekend oscillation on Saturday morning at 3 o'clock, the 123th hour.

$$c_8 = -0.25\pi + d_{first} \cdot \frac{2\pi}{7} \quad (12e)$$

The amplitude of the weekly oscillation has a significant dependence on the power consumption in the industrial sector, $E^{j_{ind}}$. The more a region is industrialised, the less pronounced is the difference between weekdays and weekends.

$$a_8 = 0.063263 \cdot E_{ind}^j \cdot E_{ave}^{tj} \quad (12f)$$

Where $E^{j_{ind}}$ is the industry factor, the power consumption in industrial sector and $E^{tj_{ave}}$ is the average electricity consumption over the year.

3.5.2 Double frequency of week oscillation

The basic week oscillation would stress too much the Wednesday, so that the oscillation of the 3.5 day period and half of the amplitude corrects the Wednesday and the minimum value is further emphasised.

$$y_9 = a_9 \sin^{n_9} (b_9 x + c_9) + d_9 \quad (13)$$

$$d_9 = 0 \quad (13a) \quad n_9 = 1 \quad (13b)$$

$$a_9 = \frac{a_8}{2} = 0.032 \cdot E_{ind}^j \cdot E_{ave}^{tj} \quad (13c)$$

$$b_9 = \frac{2\pi}{8760} \cdot \frac{365}{7} \cdot 2 \quad (13d)$$

$$c_9 = -2 \cdot c_8 - \frac{3}{2}\pi = -\pi - 2 \cdot d_{first} \cdot \frac{2\pi}{7} \quad (13e)$$

3.6 Weekend oscillation

3.6.1 Basic weekend oscillation

To take into account the difference between weekdays and weekends another set of oscillations is used. With $k_l \in \mathbb{N}, [1,52]$ we get

$$\text{For } x_w^1 \in \left[\frac{124 - (d_{first} - 1) \cdot 24 + (k_1 - 1) \cdot 24 \cdot 7}{172 - (d_{first} - 1) \cdot 24 + (k_1 - 1) \cdot 24 \cdot 7} \right]$$

It is assumed that weekend starts at 5:00 on Saturday and ends at 3:00 on Monday. For countries with the weekend on Friday and Saturday x_w defined as follows:

$$x_w^2 \in \left[\frac{100 - (d_{first} - 1) \cdot 24 + (k_1 - 1) \cdot 24 \cdot 7}{148 - (d_{first} - 1) \cdot 24 + (k_1 - 1) \cdot 24 \cdot 7} \right]$$

It is assumed that weekend starts at 5:00 on Friday and ends at 3:00 on Sunday.

$$y_{10} = a_{10} \sin^{n_{10}} (b_{10} x + c_{10}) + d_{10} \quad (14)$$

with $x \in \mathbb{N}, x_w^1, x_w^2$.

$$d_{10} = 0 \quad (14a) \quad n_{10} = 1 \quad (14b)$$

The length of the period is equivalent to the length of the period of the basic diurnal period.

$$b_{10} = b_4 = \frac{2\pi}{8760} \cdot 365 \quad (14c)$$

A sinusoidal oscillation is shifted by a half period to weaken the amplitude of the basic diurnal period.

$$c_{10} = c_4 + \pi = 2.9 \cdot \frac{2\pi}{24} \quad (14d)$$

The industrial activity has the dominating influence on the difference between weekdays and weekend demand oscillations. The higher the industrial share in the total demand, the more the weekly spread is reduced.

$$a_{10} = (a_4 - a_5) \cdot E_{ind}^j = E_{ind}^j \cdot 0.12 \cdot E_{ave}^{tj} \left(\left(1 - e^{-\frac{-GDP_{cap}^{tj}}{10}} \right) - (E_{hng}^{tj})^8 \cdot f_{a_3}^4(E_{hng}^j) \right) \quad (14e)$$

Where E_{ind}^j is the industry factor, i.e. relative the power consumption of the industrial sector.

3.6.2 Double frequency of weekend oscillation

To reduce the daily amplitude of the load curve over the weekend, it is also necessary to reduce the double daily frequency during that period.

$$y_{11} = a_{11} \sin^{n_{11}}(b_{11}x + c_{11}) + d_{11} \quad (15)$$

with $x \in \mathbb{N}$, x_w^1 , x_w^2 (for x_w^1 and x_w^2 see section 3.6.1)

$$d_{11} = 0 \quad (15a) \quad n_{11} = 1 \quad (15b)$$

$$b_{11} = b_6 = \frac{2\pi}{8760} \cdot 365 \cdot 2 \quad (15c)$$

$$c_{11} = c_6 + \pi = -24.2 \cdot \frac{2\pi}{24} \quad (15d)$$

$$a_{11} = a_6 \cdot E_{ind}^j = 0.044 \cdot E_{ind}^j \cdot E_{ave}^{tj} \left(\left(1 - e^{-\frac{-GDP_{cap}^{tj}}{10}} \right) - (E_{hng}^{tj})^8 \cdot f_{a_3}^4(E_{hng}^j) \right) \quad (15e)$$

Where E_{ind}^j is the industry factor.

3.6.3 Decreased weekend average

The average demand on weekends is lower than on weekdays, which needs to be adjusted.

$$y_{12} = a_{12} \sin^{n_{12}}(b_{12}x + c_{12}) + d_{12} \quad (16)$$

with $x \in \mathbb{N}$, x_w^1 , x_w^2 (for x_w^1 and x_w^2 see section 3.6.1)

$$a_{12} = 0 \quad (16a) \quad b_{12} = 0 \quad (16b) \quad c_{12} = 0 \quad (16c) \quad n_{12} = 1 \quad (16d)$$

$$d_{12} = 0.136493 \cdot E_{ave}^{tj} \cdot \left(1 - e^{-\frac{E_{ind}^j}{0.55691}} \right) \quad (16e)$$

Where E_{ave}^{tj} is the average electricity consumption over the year and E_{ind}^j is the industry factor.

3.7 Afternoon and evening peak

The Eq. (17) is introduced to account for lighting and other electricity demand correlating with activity in the dark hours of the day. We use a single sine period formulated as a \sin^2 in order to have positive values only. It begins at sunset and ends at midnight when we assume this additional demand to surcease.

$$y_{13} = \sum_{k_1=1}^{365} a_{k_1} \sin^{n_{k_1}} (b_{k_1} x + c_{k_1}) + d_{k_1} \quad (17)$$

$$d_{k_1} = 0 \quad (17a) \quad n_{k_1} = 2 \quad (17b)$$

As the sunsets occur at a different times every day, it is necessary to model 365 individual oscillations. The individual oscillations are limited to the period of the respective sunset until midnight by limiting the definition range of x (the hours of the year). The oscillations are calculated for the daily hours from 8:00 to 24:00, this time corresponds to an interval $x \in [24 \cdot (k_1 - 1) + \text{sunset}(k_1), 24 \cdot k_1]$, where $k_l \in$ the 365 days of a year.

The \sin^2 oscillation of the afternoon / evening has the period length from the time of the sunset to midnight.

$$b_{k_1} = \frac{2\pi}{2 \cdot (24 - \text{sunset}(k_1))} \quad (17c)$$

$$c_{k_1} = (24 \cdot (k_1 - 1) + \text{sunset}(k_1)) \cdot b_{k_1} \quad (17d)$$

The amplitude is dependent on the GDP per capita (GDP^{tj}_{cap}) and the time of the sunset on the specific day. In case sunset is after midnight or the sun does not set at all on a particular day its amplitude is set to zero.

$$a_{k_1} = E_{ave}^{tj} \cdot \left(0.036 - 0.036 \cdot 0.8 \cdot (\text{sunset}(k_1) - 19.5) + 0.5 \cdot e^{\frac{\ln 0.5}{6000}} \text{GDP}_{cap}^{tj} \cdot \left(1 - \frac{\text{sunset}(k_1) - 17}{24 - 17} \right) \right) \quad (17e)$$

Where E_{ave}^{tj} is the average electricity consumption over the year and GDP_{cap}^{tj} is the gross domestic product per capita.

3.8 Air conditioning

3.8.1 Day peak

If location exhibits a temperature of more than 25°C for more than 300 hours in a year, it is assumed that air conditioning is present in a significant amount. Again it is used a \sin^2 to add load.

$$y_{14} = \sum_{k_2=1}^{365} a_{k_2} \sin^{n_{k_2}} (b_{k_2}x + c_{k_2}) + d_{k_2} \quad (18)$$

$$d_{k_2} = 0 \quad (18a) \quad n_{k_2} = 2 \quad (18b)$$

$$b_{k_2} = \frac{2\pi}{24 \cdot 15} \quad (18c)$$

$$c_{k_2} = 24 \cdot (k_2 - 1) + 8 \quad (18d)$$

The period and the phase shift are modelled to have a maximum at 15:30 provided that the maximum temperature of a day exceeds 25°C.

The oscillations are calculated for the daily hours from 8:00 to 23:00, this time corresponds to an interval $x \in [24 \cdot (k_2 - 1) + 8, 24 \cdot k_2 - 1]$, where $k_2 \in$ the 365 days of a year. The amplitude is described in Eq. (18i) and applied for temperatures above 25°C.

$$f_{a_{k_2}}(T_{local\ hours}^j) = \begin{cases} 1, & \text{length}(T_{local\ hours}^j > 25^\circ \text{ C}) > 300h \\ 0, & \text{length}(T_{local\ hours}^j > 25^\circ \text{ C}) \leq 300h \end{cases} \quad (18e)$$

Basic condition:

$$\text{temp} := T_{local\ hours}^j(x \in [24 \cdot (k_2 - 1) + 8]: x \in [24 \cdot k_2 - 1]), \quad (18f)$$

where temp is temperature data vector in hourly resolution. Temp vector's values corresponds to a given hours in the interval x , $\text{temp} \in \mathbb{R}$

$$h := \max(\text{temp}) \quad (18g)$$

where h is maximum value of the $temp$ vector.

$$f_1(h) = \begin{cases} 1, & h > 25 \\ 0, & h < 25 \end{cases} \quad (18h)$$

$$a_{k_2}^1 = \frac{E_{ave}^{tj}}{900} \cdot \left(1 - e^{-\frac{-GDP_{cap}^{tj}}{10000000}}\right) \cdot \left(1 - e^{-\frac{-(f_1(h)-26)}{7}}\right) \quad (18i)$$

$$a_{k_2}(x) = a_{k_2}^1 \cdot f_{a_{k_2}}(T_{local\ hours}^j) \quad (18j)$$

Where E_{ave}^{tj} is the average electricity consumption over the year and GDP_{cap}^{tj} is the gross domestic product per capita.

3.8.2 Summer night peak

The basic assumption was made that air conditioning systems are used to a significant extent only if the temperature above 25 ° C was measured for at least 300 hours per year according to Eq. (18e).

$$y_{15} = \sum_{k_3=1}^{365} a_{k_3} \sin^{n_{k_3}}(b_{k_3}x + c_{k_3}) + d_{k_3} \quad (19)$$

for $x \in [24 * (k_3 - 1) + 1, 24 * (k_3 - 1) + 48]$, two full days, before and after the summer night.

$$a_{k_3} = 0 \quad (19a) \quad b_{k_3} = 1 \quad (19b) \quad c_{k_3} = 0 \quad (19c) \quad n_{k_3} = 1 \quad (19d)$$

Provided that summer nights have a maximum temperature exceeding 22°C between 21:00 to 8:00 additional load is set for two days adjacent to the night. Warm nights correspond to hours in the interval $x \in [24 * (k_3 - 1) + 21, 24 * (k_3 - 1) + 32]$, where $k_3 \in$ the 365 days of a year.

Basic condition:

$$temp_2 := T_{local\ hours}^j(x \in [24 * (k_3 - 1) + 21, 24 * (k_3 - 1) + 32]), \quad (19e)$$

where $temp_2$ is a temperature data vector in hourly resolution. $temp_2$ vector's values corresponds to given hours in the interval x , $temp_2 \in \mathbb{R}$

$$h_2 := \max(temp_2) \quad (19f)$$

where h_2 is maximum value of the $temp_2$ vector.

$$f_2(h_2) = \begin{cases} 1, & h_2 > 22 \\ 0, & h_2 < 22 \end{cases} \quad (19g)$$

$$d_{k_3}^1 = \frac{E_{ave}^{tj}}{1700} \cdot \left(1 - e^{-\frac{-0.038 \cdot GDP_{cap}^{tj} \cdot (f_2(h_2) - 22)}{10000}} \right) \quad (19h)$$

$$d_{k_3} = d_{k_3}^1 \cdot f_{a_{k_2}}(T_{local\ hours}^j) \quad (19i)$$

Where E_{ave}^{tj} is the average electricity consumption over the year and GDP_{cap}^{tj} is the gross domestic product per capita.

3.8.3 Winter peak

It is assumed that an air conditioning in winter exists, based on the same conditions as defiend in Eq. (18e). However, it is also assumed that no other form of heating exists, if the minimum temperature does not fall below 2 °C and that the air conditioning is used as heating on cold days through reverse cycling.

$$y_{16} = \sum_{k_4=1}^{365} a_{k_4} \sin^{n_{k_4}}(b_{k_4}x + c_{k_4}) + d_{k_4} \quad (20)$$

$$a_{k_4} = 0 \quad (20a) \quad b_{k_4} = 1 \quad (20b) \quad c_{k_4} = 0 \quad (20c) \quad n_{k_4} = 1 \quad (20d)$$

The oscillations are calculated for the daily hours from 6:00 to 23:00, this time corresponds to an interval $x \in [24 * (k_4 - 1) + 6, 24 * (k_4 - 1) + 23]$, where $k_4 \in$ the 365 days of a year.

$$f_{d_{k_4}}(T_{local\ hours}^j) = \begin{cases} 1, & \min(T_{local\ hours}^j) \geq 2 \\ 0, & \min(T_{local\ hours}^j) < 2 \end{cases} \quad (20e)$$

Additional restriction for this oscillation checks that daily average temperature should fall below 15 °C.

$$temp_3 := T_{local\ hours}^j(x \in [24 * (k_4 - 1) + 1, 24 * k_4]), \quad (20f)$$

where $temp$ is temperature data vector in hourly resolution. $Temp_3$ vector's values corresponds to a given hours in the interval x , $temp_3 \in \mathbb{R}$

$$h_3 := \max(temp_3) \quad (20g)$$

where h_3 is maximum value of the $temp$ vector.

$$f_{d_{k_4}}(h_3) = \begin{cases} 1, & h_3 < 15^\circ\text{C} \\ 0, & h_3 \geq 15^\circ\text{C} \end{cases} \quad (20h)$$

$$d_{k_4}^1 = 0.1 \cdot E_{ave}^{tj} \cdot \left(1 - e^{-\frac{-GDP_{cap}^{tj}}{10000}}\right) \cdot \left(1 - e^{-\frac{-(15-f_{d_{k_4}}(h_3))}{13}}\right) \quad (20i)$$

$$d_{k_4} = d_{k_4}^1 \cdot f_{a_{k_2}}(T_{local\ hours}^j) \cdot f_{d_{k_4}}(T_{local\ hours}^j) \quad (20j)$$

Where E_{ave}^{tj} is the average electricity consumption over the year and GDP_{cap}^{tj} is the gross domestic product per capita.

3.9 Travel and tourism contribution

Real load data shows that in countries with a strongly developed tourism sector consumption of electricity is increased during the summer period.

$$y_{17} = a_{k_5} \sin^{n_{k_5}}(b_{k_5}x + c_{k_5}) + d_{k_5} \quad (21)$$

$$a_{k_5} = 0 \quad (21a) \quad b_{k_5} = 0 \quad (21b) \quad c_{k_5} = 0 \quad (21c) \quad n_{k_5} = 1 \quad (21d)$$

The oscillations are calculated for countries, where the warmest temperature T_w^j can exceed 29 °C during the year and the tourist and travel share of the GDP_{To}^j exceeds 10.2%.

$$f_{d_{k_5}}^1(T_w^j) := \begin{cases} 1, & T_w^j \geq 29 \\ 0, & T_w^j < 29 \end{cases} \quad (21e)$$

$$f_{d_{k_5}}^2(GDP_{To}^j) := \begin{cases} 1, & GDP_{To}^j \geq 10.2 \\ 0, & GDP_{To}^j < 10.2 \end{cases} \quad (21f)$$

$$f_{d_{k_5}}^3(lat^j) := \begin{cases} 1, & lat^j \in [15, 90] \\ 0, & lat^j \in (-90, 15) \end{cases} \quad (21g)$$

The summer period corresponds to hours in the interval $x \in [24 * (k_5 - 1) + 1, 24 * k_5]$, where $k_5 \in$ the days interval which is equal to [152, 243].

$$f_{d_{k_5}}^4(x) := \begin{cases} 1, & x \in k_5 \\ 0, & x \notin k_5 \end{cases} \quad (21h)$$

$$d_{k_5}^1 = E_{ave}^{tj} \cdot \left(1 - e^{-\frac{-GDP_{To}^j}{80}}\right) \quad (21i)$$

$$d_{k_5} = d_{k_5}^1 \cdot f_{d_{k_5}}^1(T_w^j) \cdot f_{d_{k_5}}^2(GDP_{To}^j) \cdot f_{d_{k_5}}^3(lat^j) \cdot f_{d_{k_5}}^4(x) \quad (21j)$$

Where E^{tj}_{ave} is the average electricity consumption over the year and GDP^{jTo} is the tourism and travel share in the GDP.

3.10 Maximum demand consumption

To adjust the peak load of the countries an additional function Eq. (22) is used, provided that the maximum of the target function $load(x)$ exceeds the value of $Peak^{tj}$.

$$y_{18} = a_{18} \sin^{n_{18}}(b_{18}x + c_{18}) + d_{18} \quad (22)$$

$$d_{18} = 0 \quad (22a) \quad n_{18} = 1 \quad (22b)$$

The length of the period and the phase of the shift are equivalent to the length of the period of the annual oscillations.

$$b_{18} = b_2 = \frac{2\pi}{8760} \quad (22c)$$

$$c_{18} = c_2 = 0.225 \cdot 2\pi \frac{lat}{|lat|} \quad (22d)$$

$$f_{a_{18}}^1(\max(load(x))) := \begin{cases} 1, & \max(load(x)) > Peak^{tj} \\ 0, & \max(load(x)) < Peak^{tj} \end{cases} \quad (22e)$$

The amplitude is formed by an exponential function. Countries where the warmest temperature T_w^j can exceed 40 °C during the year have the following amplitude:

$$f_{a_{18}}^2(T_w^j) := \begin{cases} 1, & T_w^j \geq 40 \\ 0, & T_w^j < 40 \end{cases} \quad (22f)$$

$$a_{18}^1 = -Peak^{tj} \cdot \left(1 - e^{-\frac{32.2 - T_{c\,month}^j}{47.9}} \right) \quad (21g)$$

The Eq (22h) defines the amplitude of the countries where the seasonal demand pattern exhibits higher consumption during winter than in summer. Therefore, the functions Eq. (6j) and Eq (6k) described in the section 3.2.1 are used to determine the amplitude of the maximum demand oscillation.

$$a_{18}^2 = -0.1335 \cdot Peak^{tj} \cdot \left(1 - e^{-\frac{12.5 - T_{c\ month}^j}{15.2}} \right) \quad (21h)$$

$$a_{18} = a_{18}^1 \cdot f_{a_{18}}^1(\max(load(x))) \cdot f_{a_{18}}^2(T_w^j) + a_{18}^2 \cdot f_{a_{18}}^1(\max(load(x))) \cdot f_{a_2}^4(T_{c\ month}^j) \cdot f_{a_2}^5(lat^j) \quad (22i)$$

Where $Peak^{tj}$ is the maximum electricity demand for the years 2017 to 2100 and $T_{c\ month}^j$ is the average temperature of the coldest month.

3.11 Calibration total annual demand

The total annual demand is an input variable to the model and this last summand ensures that the integral of the annual load matches the total annual demand. To maintain the annual electricity demand a bias constant is applied over all hours of the year.

$$Error = \frac{E_y^{tj} - \sum_i y_i(x)}{8760} \quad (23)$$

$$load(x) = \sum_i y_i(x) + Error \quad (24)$$

$$E_y^{tj} = \int_1^{8760} load(x) dx \quad (25)$$

Where E_y^{tj} is the annual electricity consumption, y_i is the sum of sine functions (i denotes the number of sine functions), $Error$ is the mean absolute error and $load(x)$ is the hourly synthetic electricity demand.

3.12 Estimation of future electricity demand and load profile

The model introduced in this section is well suited for founded estimates of the future electricity demand and the respective hourly demand profile for all countries in the world. The future electricity demand of countries is estimated by applying the model to an assumed future economic development level and related variables, such as electricity demand, peak load and GDP per capita as described in the data section. It is assumed that these explanatory variables are most important for the electricity demand and the load profile in long-term projections.

4. RESULTS AND APPLICATION

4.1 Modeled load curve quality

The accuracy of the proposed model is tested using hourly actual load values in hourly resolution as presented in the Appendix (Table A1). An error analysis, based on the R-squared error, is provided, in order to estimate the model performances and their reliability. The R-squared error is calculated as follows:

$$R^2 = 1 - \frac{SSE}{SST} \quad (26)$$

where SSE is the sum square error and SST is the sum of squared total. These performance measures are defined as;

$$SSE = \sum_{i=1} (\text{load}_{r i} - \text{load}_{m i})^2 \quad (27)$$

$$SST = \sum_{i=1} (\text{load}_{r i} - \overline{\text{load}_i})^2 \quad (28)$$

where $\text{load}_{r i}$ and $\text{load}_{m i}$ denote the real actual values and modeled values of the load respectively for the i -th hour. The $\overline{\text{load}_i}$ shows the average value of the hours of each day of the year.

The R-squared errors for 56 countries with available real load data are illustrated in Figure 7. The R-squared error values show satisfactory results.

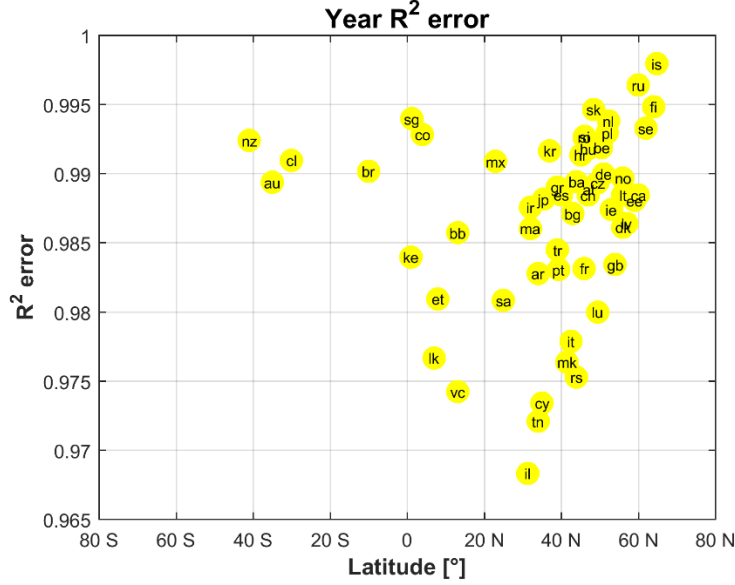


Fig. 7. Values of R-squared error for countries with real load data. Abbreviations of countries are due to their internet endings.

The error values for all countries with real load profile are summarised in the Appendix (Table A2).

4.2 Modeled peak load quality

To evaluate the modeled peak load quality, the actual peak load has been compared to model peak load results. The deviation (Dev) is provided as a measure of accuracy of the model for reproducing the peak load and defined as follow:

$$Dev = \left[\frac{Peak_m - Peak_r}{Peak_r} \right] \cdot 100 \quad (29)$$

where $Peak_m$ and $Peak_r$ are the modelled and real values of the load peak respectively. Figure 8 illustrates the peak load deviation. 41 % of the countries with real peak load data have peak load deviations within an error bar of $\pm 5\%$. As can be observed in Figure 8, countries with electricity consumption varying between 300 and 5000 TWh have the smallest peak deviation, it means synthetic peak values are close to real peak load.

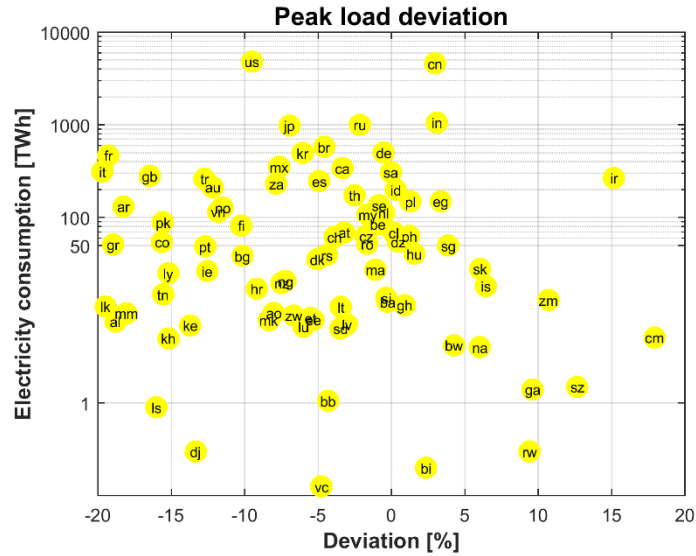


Fig. 8. Peak load deviation.

The deviations of the modeled and real load peaks are provided in detail in the Appendix (Table A3).

4.3 Model results for exemplarily countries and special impact variables

4.3.1 Impact variables

It was detected that specific economic, technical and climate characteristics have a significant influence on the quality of the results.

4.3.1.1 Tourism factor

The impact of the tourism on electricity demand was examined for the example of Cyprus, where the share of tourism and travel in GDP equals 19.3%. It can be seen from Figure 9 that lack of tourism impact in the model for Cyprus leads to growth of modelling error during the summer. The peak load deviation increased by 1.3%, i.e. the peak load with and without the tourism factor is 689 MW and 601 MW, respectively, compared to the real peak load of 954 MW. As it is depicted in the Figure 9, the histogram of the modelling error is almost symmetrical around to the zero of the ordinate axis. However, the modelling error increases without tourism factor and leads to a different appearance in the shoulders of histogram.

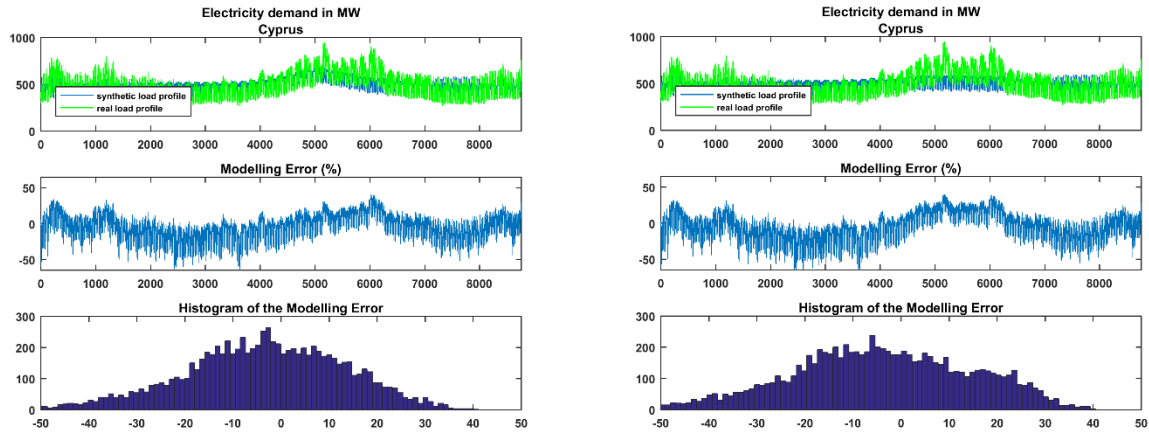


Fig. 9. Actual load data and synthetic load data (i), the modelling error (ii) histogram of the modelling error (iii) for Cyprus in the year 2015 with (left) and without (right) tourism impact.

4.3.1.2 Industrial production factor

Electricity consumption depends also on industrial production. In Russia, where 52% of total electricity consumption is industrial electricity consumption, this impact is significant. Figure 10 shows the actual and the synthetic load profiles, the modelling error and histogram of the modelling error for Russia in the year 2014. It can be noticed that the amplitude of the synthetic load significantly exceeds the real load amplitude. The graphical representation of the error illustrates the influence of the industrial impact on the load observed during the year. The difference between histograms of the modelling error with and without industrial production impact is huge. It can be explained by the magnification of the modelling error range due to the removal of the industrial production factor. The peak load deviation increased by 2.0%, i.e. the peak load with and without the industrial production factor is 151 GW and 161 GW, respectively, compared to the real peak load of 155 GW. The main explanation of the high relevance of this factor is that industrial demand is more close to baseload due to 24/7 production conditions compared to a much higher relative demand during daytime and evening hours of private households, but also for commercial demand, such as retailers and many service businesses. Hence the higher the industrial demand in the overall power sector the less pronounced is the relative minimum and maximum load compared to the daily average.

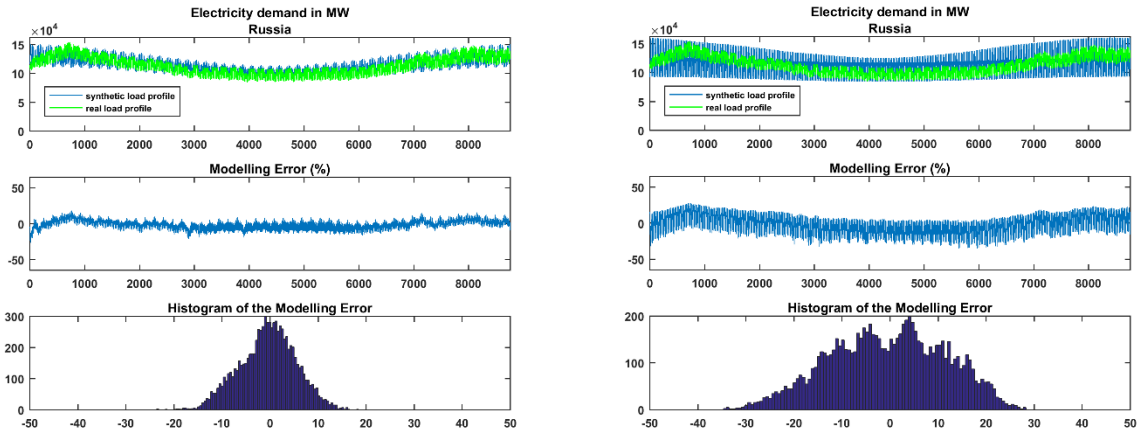


Fig. 10. Actual load data and synthetic load data (i), the modelling error (ii) histogram of the modelling error (iii) for Russia in the year 2014 with (left) and without (right) industrial production impact.

4.3.1.3 Air conditioning factor

Weather and climate conditions represent the most influential exogenous variables. Temperature is the most commonly used weather variable. Air conditioning in Japan as an example of the temperature influence is examined in the following. An increasing modelling error for the period between hours 3000 and 6000 can be observed based on the histograms in the Figure 11. The elimination of air conditioning impact leads to an increased peak load deviation from -6.9% to -17%.

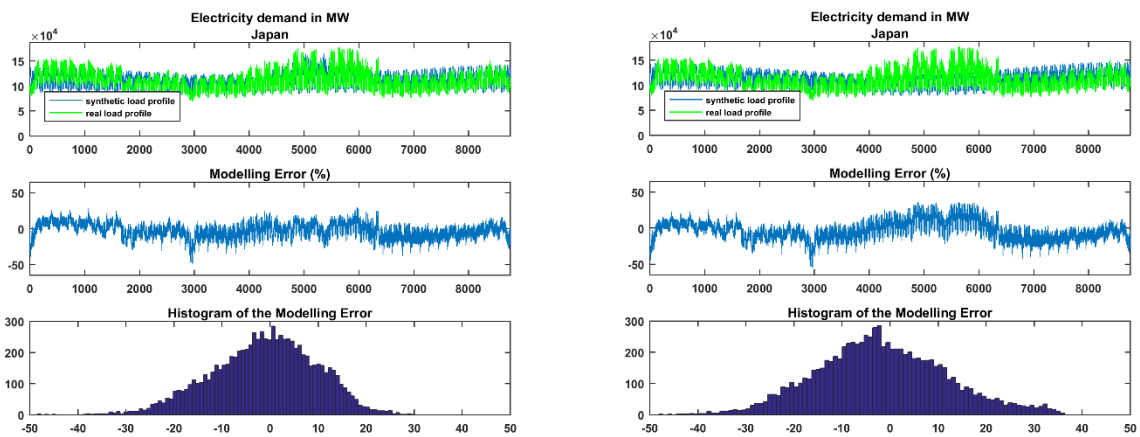


Fig. 11. Actual load data and synthetic load data (i), the modelling error (ii) histogram of the modelling error (iii) for Japan in the year 2015 with (left) and without (right) air conditioning impact.

4.3.1.4 Electric heating factor

The ratio of electricity sourced from hydro, nuclear and geothermal power to total generated electricity in France is 89%. The inflexible nuclear baseload generation leads to electric heating systems which can use the excess electricity in the night hours, often stored for the following day, leading to a strong temperature sensitivity of the French power sector. Figure 12 shows that the distribution of the modelling error in the histogram deviates towards negative values. This implies that the values of the real profile exceed the synthetic load values because of the elimination of the electric heating impact. The R-squared error increased from 0.97 to 0.98 by introduction electric heating factor. In addition, the elimination of electric heating impact leads to an increased peak load deviation by 1.3%.

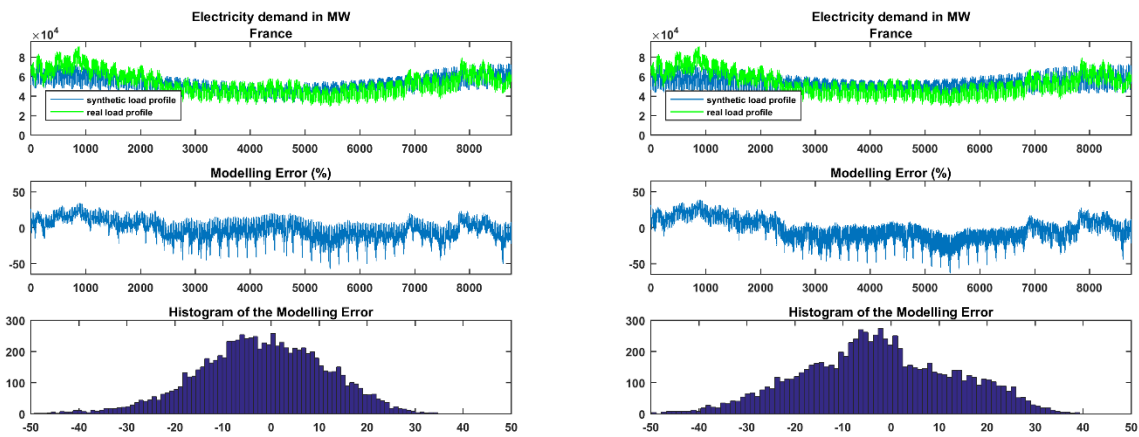


Fig. 12. Actual load data and synthetic load data (i), the modelling error (ii) histogram of the modelling error (iii) for France in the year 2015 with (left) and without (right) electric heating impact.

4.3.1.5 Sunset hours factor

The time factor, such as sunset hours, affect the electricity demand. The influence of sunset hours is shown for the example of New Zealand. As depicted in Figure 13, the exclusion of sunset hours for New Zealand results in an increase in the modelling error for the period between hours 3000 and 5000. The peak load deviation is increased from -7.5% to -17.5%.

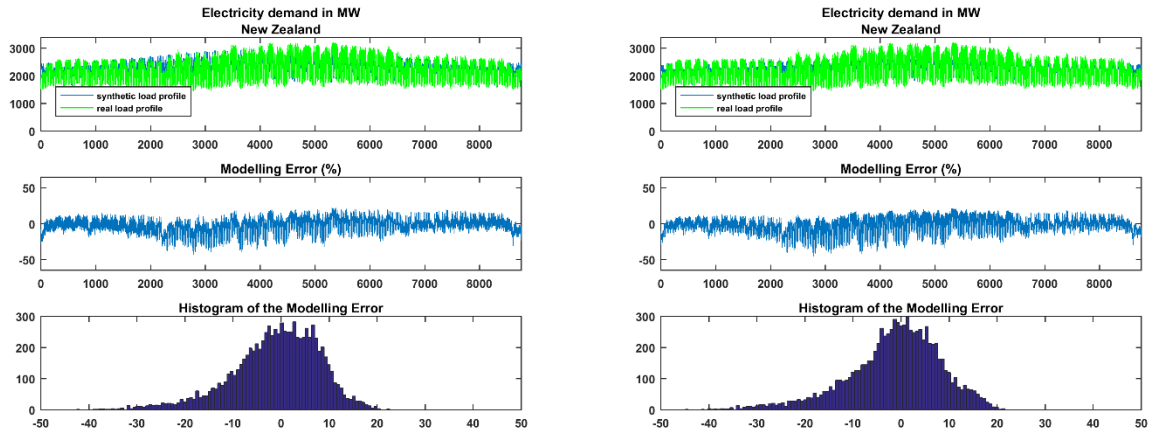


Fig. 13. Actual load data and synthetic load data (i), the modelling error (ii) histogram of the modelling error (iii) for New Zealand in the year 2015 with (left) and without (right) sunset hours impact.

4.3.2 Sweden

In Figure 14 the model results are presented for the example of Sweden and the harmonics of the annual, diurnal and weekly variations for the year 2015 are displayed. The synthetic load demand achieves a R-squared error of 99% and the peak deviation is 0.8% compared to the actual peak. The electrical load pattern in the country varies for the different seasons. The electricity consumption is highest in January, and lowest during the holiday season in August.

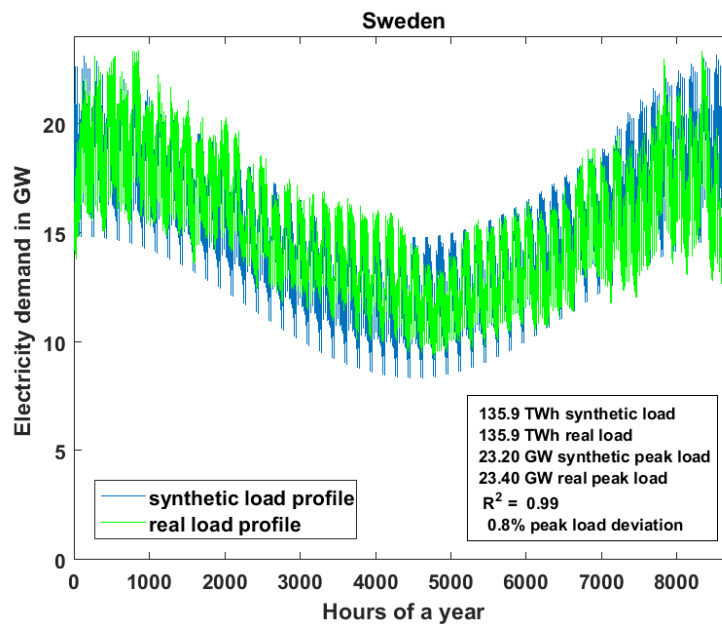


Fig. 14. The synthetic and the actual demand of Sweden for the year 2015.

Figure 15 presents the synthetic and the actual demand of Sweden for the year 2015 as matrix for all 8760 hours in a resolution for the 365 days and the 24 hours. The graphs for the actual and synthetic load show the daily minimum in the early morning hours of the night at around 3:00. Furthermore, both graphs demonstrate two load peaks, one around noon and the second in the early evening around 19:00. In the winter months, the evening peak is substantially higher than the noon peak, whereas in summer months the peaks are very similar. It can be seen from the actual error plot that the maximum value of the absolute error is -7 GW, equal to -48%. 47% of the load deviations are within an error bar of $\pm 5\%$.

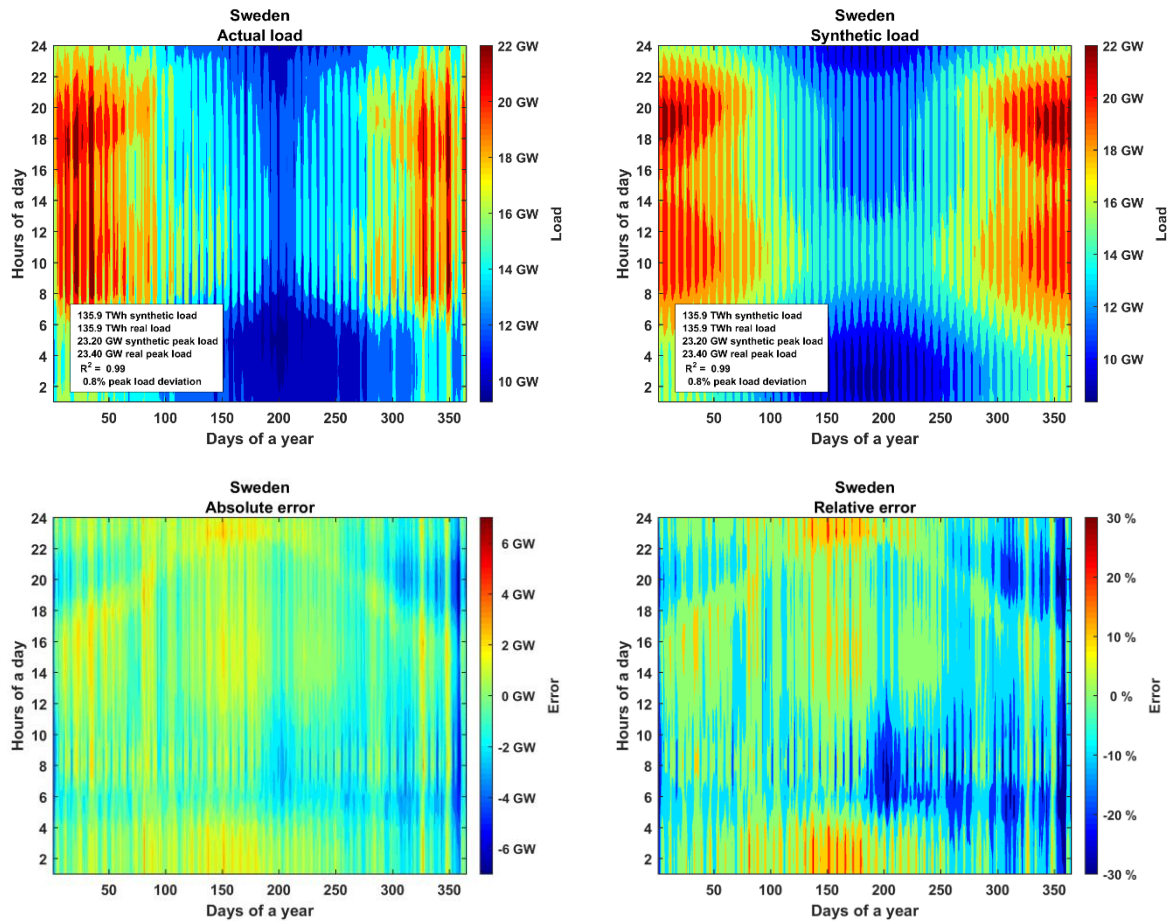


Fig.15. Actual load data (top, left), synthetic load data (top, right), absolute error (bottom, left) and relative error (bottom, right) for Sweden in the year 2015.

Figure 16 shows for the resolution of one week in October that both weekday and weekend intraday variations are faithfully reproduced. The weekly demand profile exhibits lower consumption during weekends. The peak demand switches from one peak in the late morning to a weaker peak in the afternoon.

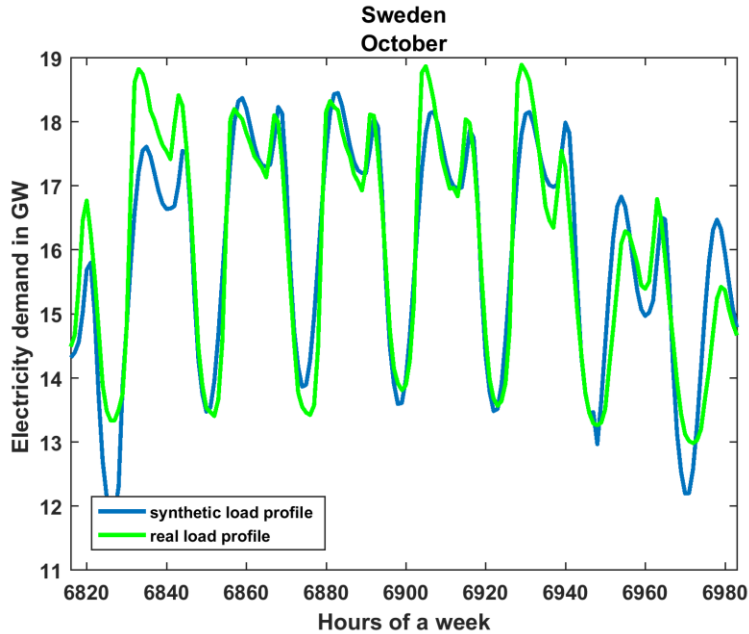


Fig. 16. The synthetic and the actual demand for Sweden in the year 2015, for a representative week in October.

Figure 17 illustrates that the overall performance of the model is good for the example of Sweden. However, a closer look on Figure 12 indicates that the model values diverge more from the actual values in the modelled load region between 20 GW to 25 GW. At lower temperatures it is observed that the deviation of modelled values from the actual values is more significant. Warm summer days also show deviations since the model tends to project too low load values compared to the fact that the Swedish power system does not tend to show load values significantly below 1 GW.

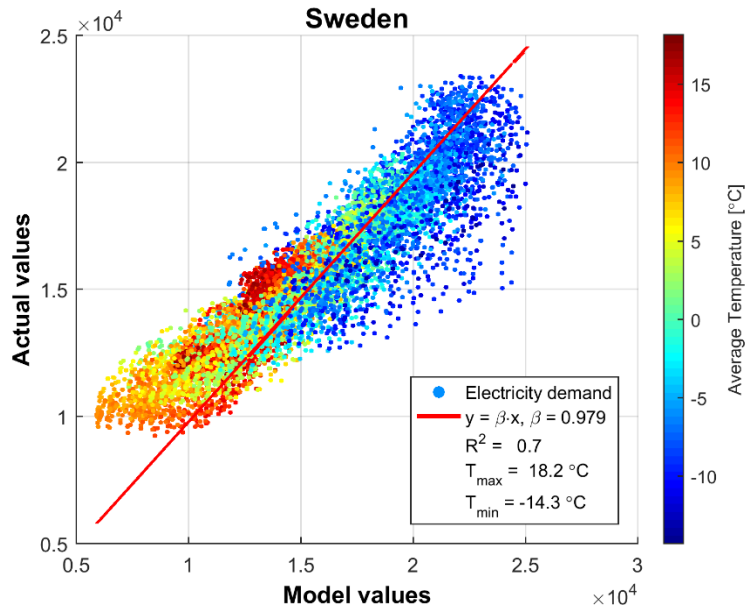


Fig. 17. The model performance for Sweden and the year 2015 depending on temperature.

Figure 18 depicts that the model is satisfactory for the example of Sweden. The graphical representation of the error is empirically reliable. The histogram shows the relative error sorted into a certain interval of error values. It can be seen from Figure 18 that the distribution is almost symmetrical around to the zero error.

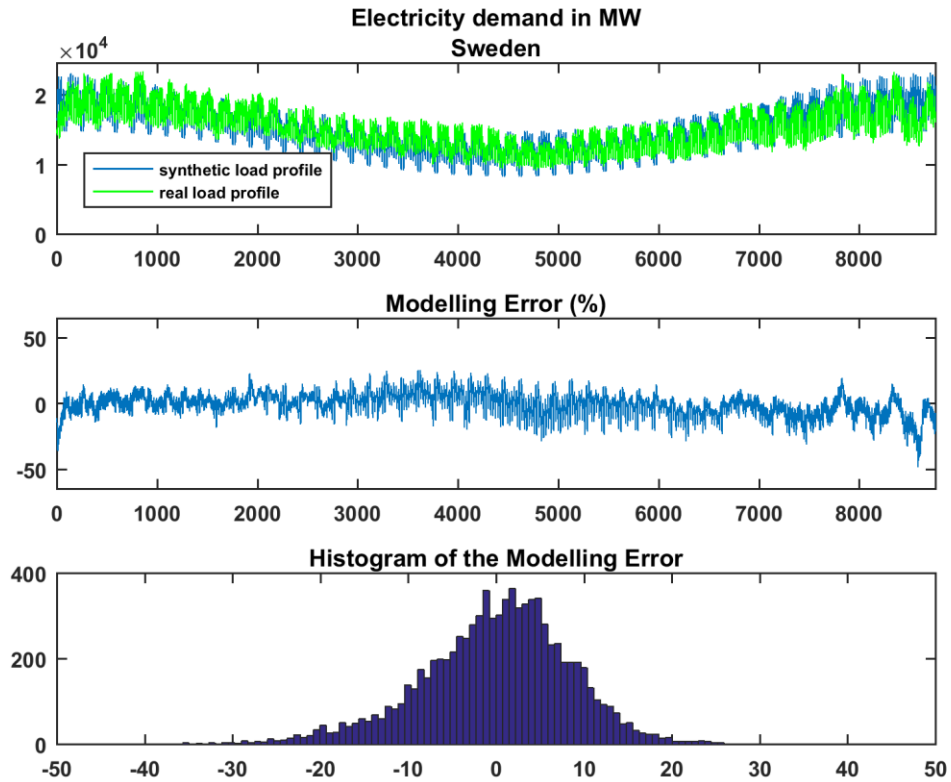


Fig. 18. Actual load data and synthetic load data (i), the modelling error (ii) histogram of the modelling error (iii) for Sweden in the year 2015.

4.3.3 Iran

Forecasts have been created for annual electricity demand by applying the assumption of section 2.3. Figure 19 shows modeled values of annual electricity demand for the example of Iran for the years 2017 - 2100. The logistic growth of the electricity consumption can be observed reaching a plateau level at around the year 2070.

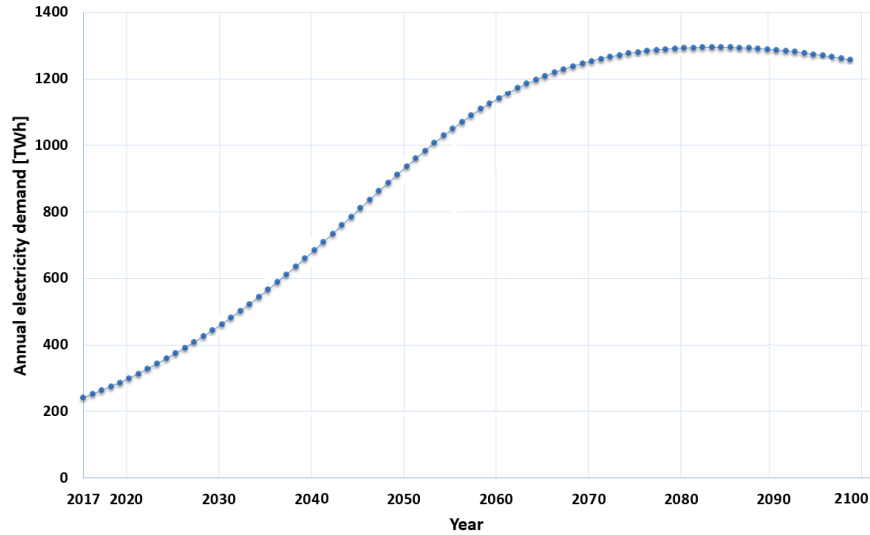


Fig. 19. The synthetic annual demand of Iran for the years 2017 - 2100.

The synthetic and the actual electricity demands of Iran for the year 2015 are presented in Figure 20. It can be seen from Figure 20 that the consumption is highest in the summer period. There is a strong divergence between the curves in March. This is because the model does not include the influence of religious and public holidays. The Iranian New Year falls between 20 March and 24 March. The holidays last 5 days in general and 14 days for schools and universities resulting in an decrease in electricity demand during this period.

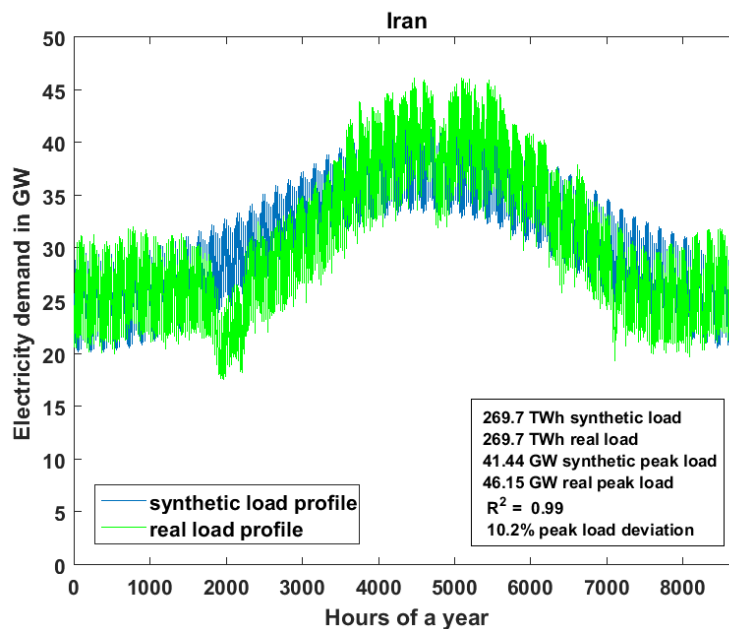


Fig. 20. The synthetic and the actual demand of Iran for the year 2015.

Figure 21 illustrates the actual load, the synthetic load, absolute error and relative error as matrix for all 8760 hours in a resolution for 365 days and daily 24 hours, for the year 2015. The increased demand during the summer can be easily observed from the actual load and the synthetic load graphs. In winter it can be noticed that the evening peak is higher than the noon peak in both graphs. The maximum of the errors is observed during the Iranian New Year, due to religious and public impacts not being included in the model. 35 % of the load deviations are within an error bar of $\pm 5\%$.

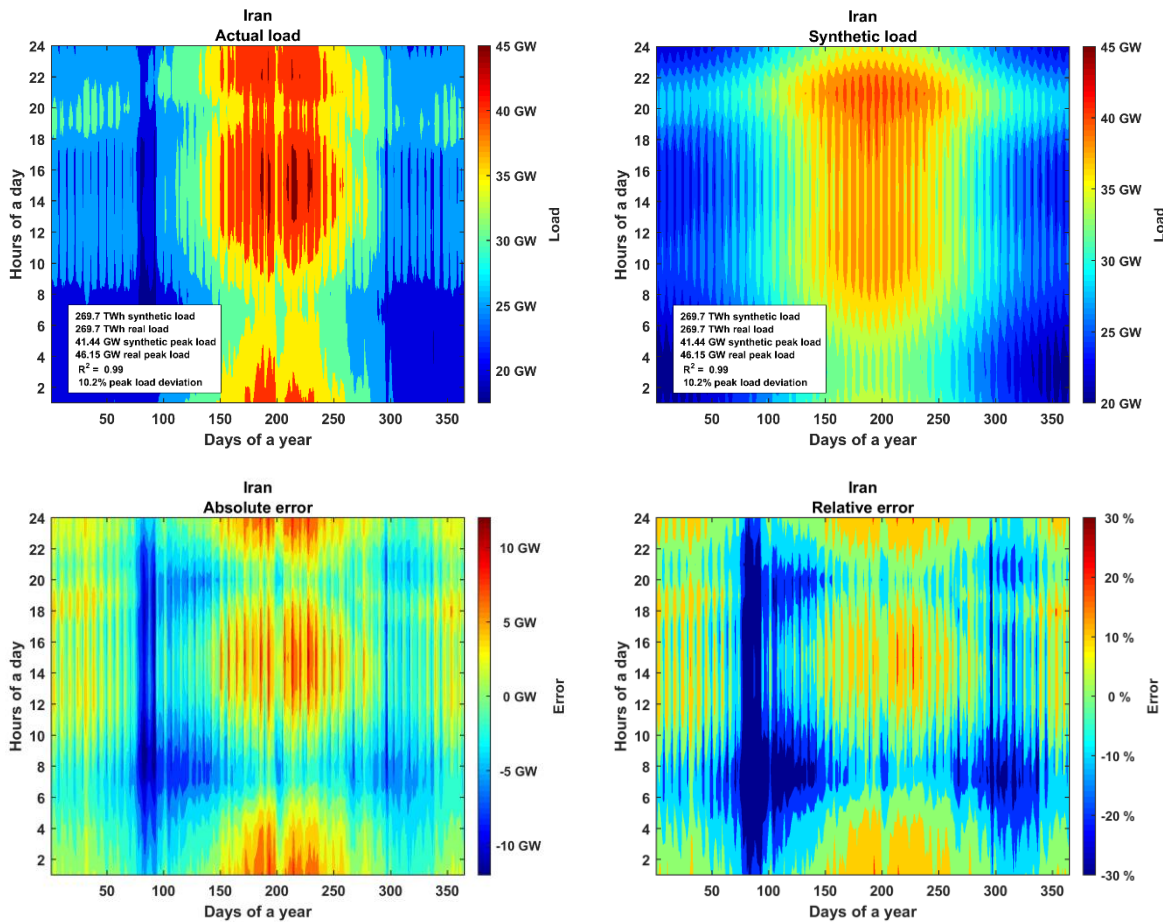


Fig. 21. Actual load data (top, left), synthetic load data (top, right), absolute error (bottom, left) and relative error (bottom, right) for Iran in the year 2015.

The October week is illustrated in Figure 22. This shows the magnitude of the weekly and daily load curves. The load decreases on Thursday, Friday and the night hours of all weekdays. Weekend

in Iran is Thursday and Friday, the model takes correctly into account decreasing load during the Iranian weekend.

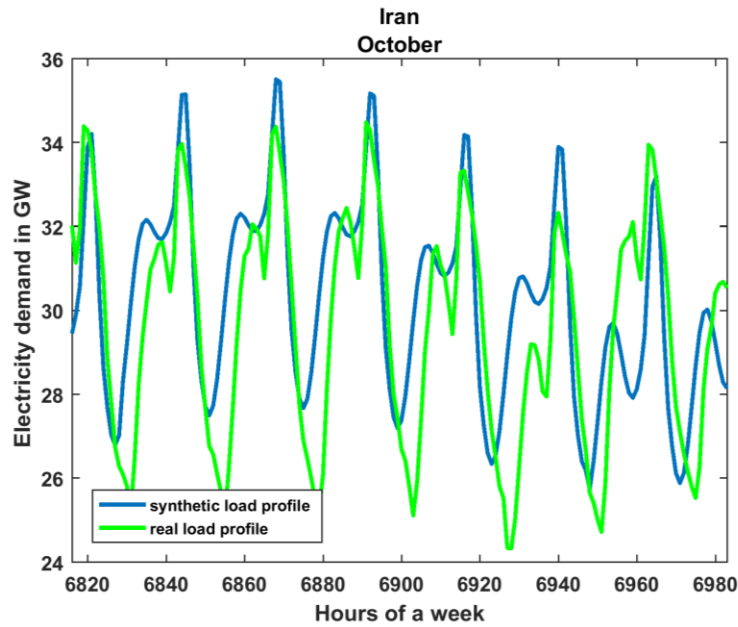


Fig. 22. The synthetic and the actual demand for Iran in the year 2015, for a representative week in October.

Figure 23 presents the performance of the model in case of Iran for the year 2015. The maximum mismatch of loads is observed at minimum temperatures from 0 to 5 °C.

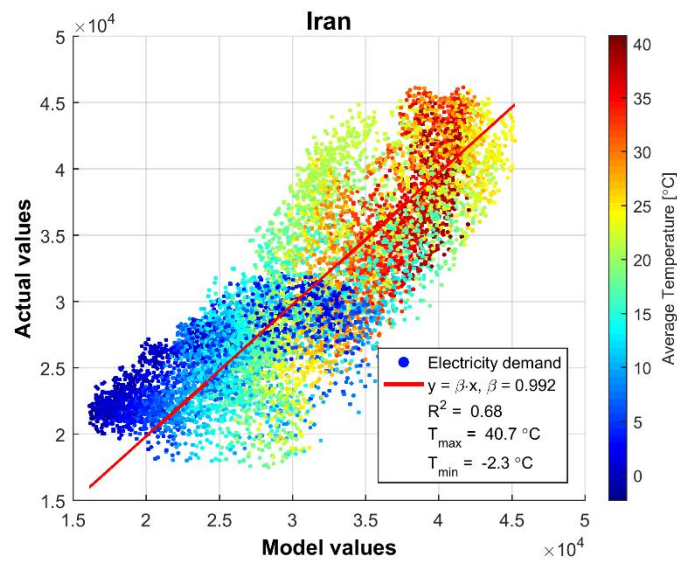


Fig. 23. The model performance for Iran and the year 2015 depending on temperature.

Figure 24 illustrates the actual and synthetic load profiles, the modelling error and histogram of the modelling error. The difference in the shoulders of the histogram and the increase of the modelling error during March can be explained by the exclusion of holidays in the model.

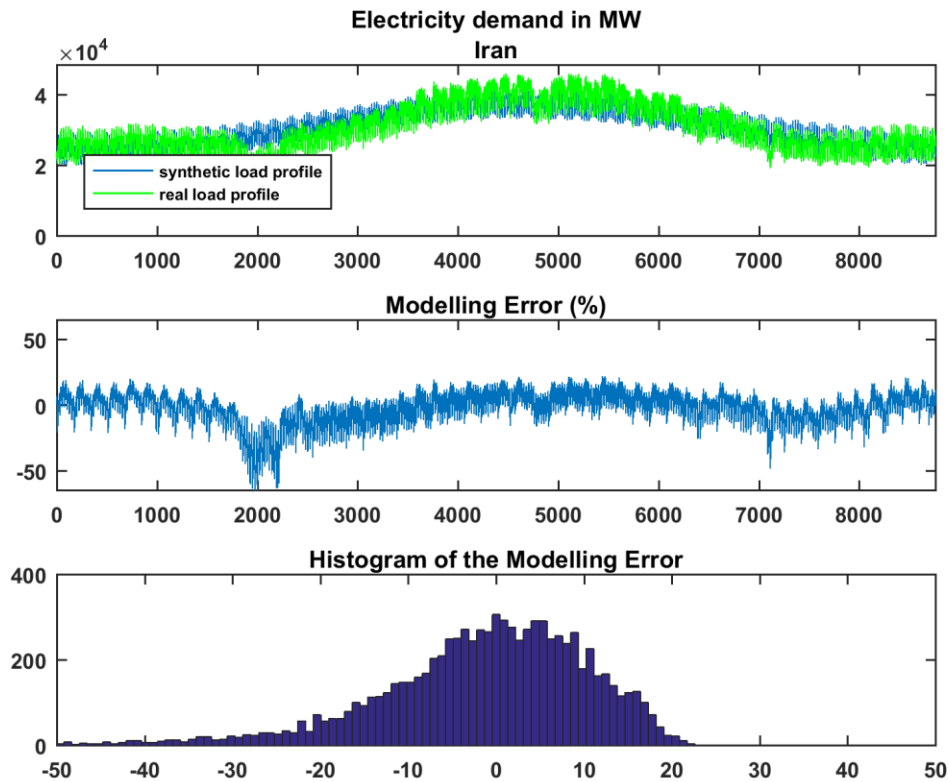


Fig. 24. Actual load data and synthetic load data (i), the modelling error (ii) histogram of the modelling error (iii) for Iran in the year 2015.

All results for countries with real load and peak data can be found in the appendix.

4.4 Forecast of electricity demand and the respective load profile

The introduced model allows to estimate the annual electricity demand and its hourly resolution for all countries based on available data and assumptions for the period from 2017 to 2100. Estimates for the annual electricity demand for all countries in the world are presented for the years 2015, 2030, 2050 2070 and 2090 in the Appendix (Table A4). Projections of the hourly electricity

consumption as matrix for 8760 hours in a resolution for 365 days and daily 24 hours are presented for all countries, regions, continents and the world for the year 2030 in the Appendix (Table A5).

The model results are compared to the findings of Finnish researchers on the future Finnish electricity consumption in a baseline and vision scenario used by the Finnish Ministry of Employment and the Economy [41]. The results are presented in Table 2 and Figure 13.

Table 2. Finnish electricity demand scenarios in TWh. Data for 2010 is historic data, for 2015 the projected data of the two VTT scenarios is shown and the historic demand for the case of this model.

Scenarios	2010	2015	2020	2030	2040	2050	2060	2070	2080	2090	2100
VTT baseline	87.5	98.1	103	108	113	116					
VTT vision	87.5	98.1	99	95	90	80					
this model	87.5	82.3	84.7	92.5	99.3	101.5	101.8	102.7	104.5	105.3	105.6

From the Figure 25 it can be seen that all three scenarios differ, in particular the VTT baseline and VTT vision scenario which projects two diametrical trends, as business-as-usual case and a scenario based on either very high efficiency gains or drastic economic decline. The scenario of this research is comparable to the business-as-usual scenario but shifted to lower values. The scenario of this research shows an increasing trend till 2040/2050 and then a saturated plateau till the end of the century.

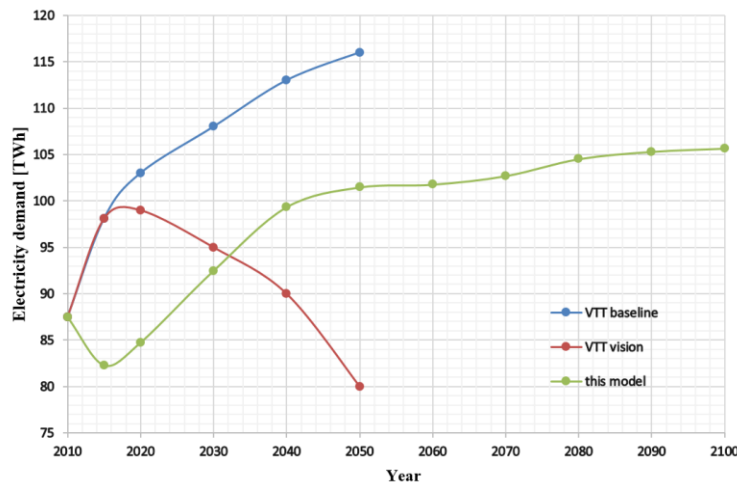


Fig. 25. Finnish electricity consumption scenarios.

Figure 26 depicts relatively constant seasonal pattern of the electricity consumption throughout the presented years for the case of Finland. It can be observed that electricity consumption is higher during the winter months. The diurnal electricity demand pattern shows a peak demand close to noon and in the evening for all years.

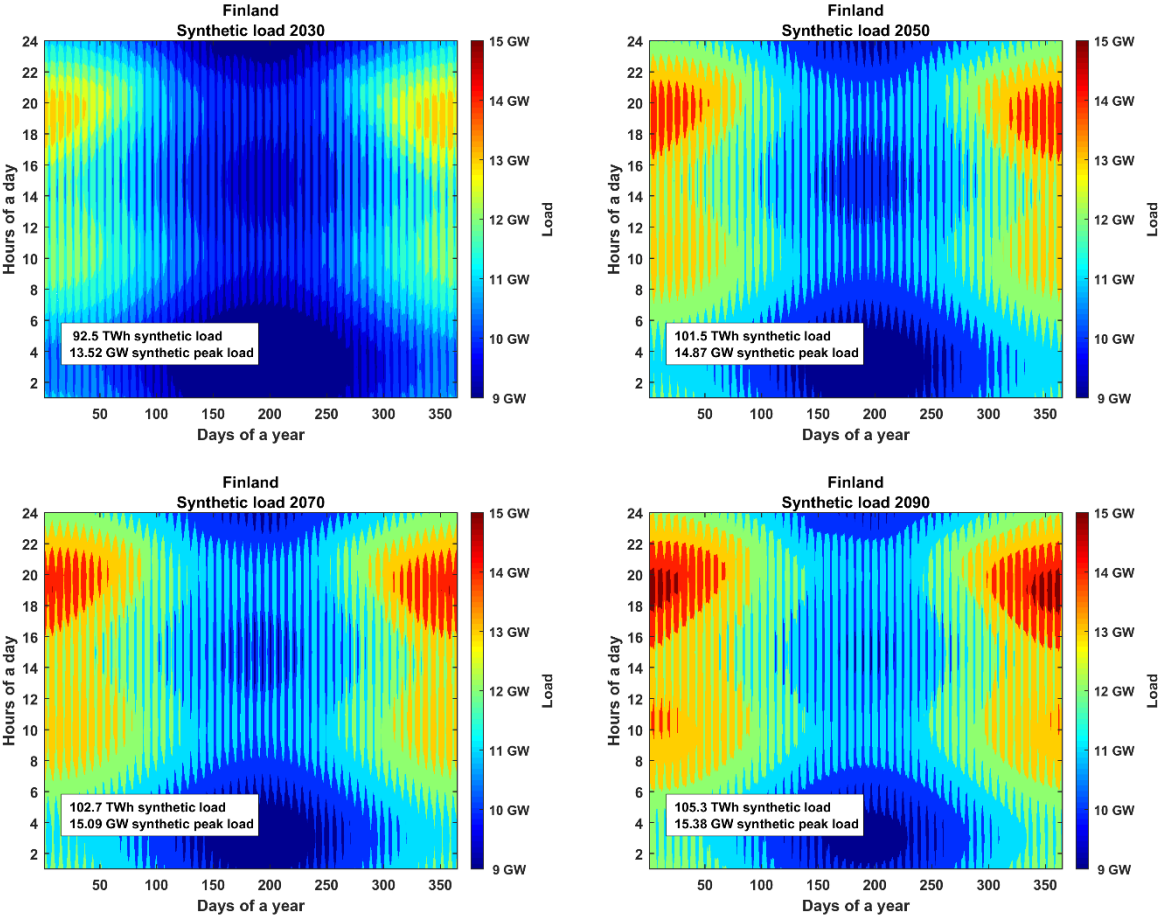


Fig. 26. The synthetic hourly electricity demand of Finland for the years 2030, 2050, 2070 and 2090.

5. DISCUSSION

A long-term electricity forecasting model, based on the relationship between the electricity load and the relevant driving parameters, has been developed in this paper. In the model the most commonly discussed driving parameters, such as existing load data, economic data, annual electricity consumption, annual peak load, temperature and some country-specific economic data are applied [27]. In addition to the common parameters mentioned in literature, new parameters such as the time of sunset, tourism, travel share in GDP and proportion of the electricity generation share of hydro, nuclear and geothermal power plants are introduced.

The main difference between the proposed model and other multiple regression models [3,6-13] is that the electricity demand forecast is developed in an hourly resolution, not annual. However, research about modelling and forecasting demand in hourly resolution is being increasingly discussed in literature [2,6,11]. The main focus in the literature is on modelling the demand of one specific country and authors suggest to apply a similar methodology for other countries. In this research a forecasting model is proposed that can be used for all countries globally. Furthermore, in contrast to other studies, the approach projects an electricity demand forecast for the period from 2017 - 2100.

The historical hourly load data of 47 countries [44-86] all around the world are compared with the modelled results for the same years to verify the results or the thus calibrated model parameters. The R-square error values for the modelled and actual loads vary between 0.968 – 0.998. It was found that specific economic, technical and climate characteristics, such as high shares of marginal cost generation, air conditioning, impact of tourism and industrial consumption, local temperature and seasonal effects have significant influence on the quality of results. For example in Cyprus, one of the countries with a high share of the touristic sector of the total GDP, it can be seen that if the tourism and travel share in GDP is not taken into account in the model, the modelling error of Cyprus is significantly increased during summer.

Meanwhile, the industrial consumption impact on electricity demand pattern can be observed in Russia. Without this factor, the peak deviation of the model changes from -2.1% to 4.1%. The

proportion of the electricity generation share of hydro, nuclear and geothermal power plants has a major impact on the results for France, where the electricity generation share of hydro, nuclear and geothermal is equal 0.89, mainly driven by nuclear energy. The resulting R-square error varies between 0.97 and 0.98 depending on the inclusion of this parameter. Another important parameter is the influence of air conditioning on the electricity demand pattern. In countries such as Japan where air-conditioning is used heavily, the peak load deviation of synthetic load increased from -6.9% to -17%. For New Zealand the impact of sunset hours leads to a larger modelling error in the winter.

Based on the obtained results of the case countries Sweden and Iran, it is obvious that the model shows satisfied synthetic load profiles for countries with different geographic, socio-economic, climatic and technical conditions. The synthetic load demand achieves a R-squared error of 99% for both countries. It means that despite the high availability of the real load profiles for European countries and less for emerging and developing countries the model shows appropriate results for diverse countries without a bias towards developed countries. The strong impact of temperature is also covered well for the case of Iran.

The proposed electricity demand model, based on only a few easily accessible parameters, is the very first model that is applicable to all countries globally. The model can be also used to project the future electricity demand and the respective load profile. This makes the model in particularly relevant for energy scenario research which increasingly requires not only a projection for the annual electricity demand, but also a hourly resolution for entire years due the increasing share of variable renewable energy generation all around the world.

Long-term electricity demand forecasting is a crucial part for planning and expansion of electric power systems [1]. In fact, it plays an essential and important role on the planning for the construction of new generation facilities. The obtained results could have a significant impact and support in energy transition studies towards sustainability. The results of this work can be applied to power network planning, and power networks can be analysed by this methodology for a long time period.

Future research dedicated to further improvements may be related to introduce a new temperature profile taking temperature increase due to climate change into account. In addition good data on country-wide vacation periods, holiday seasons and religious and cultural events may also further improve the model. Future energy technologies can have an influence on the electricity demand in the future. For instance, energy storage can decrease peak power demand while electric vehicles can increase the peak power demand. Electric vehicles will very likely penetrate the markets on a large scale in the future and will increase the electricity demand. Impact of the heating and cooling load on electricity demand pattern could be considered in more detail to improve the predictability of the model. Electricity consumption varies considerably between different types of buildings. For instance, in detached houses, more electricity is usually consumed per square meter compared to flats. Moreover the buildings structure, the heating and cooling systems and the growth of area demand per capita in houses as a consequence of increasing GDP could be taken into account in future research.

Distributed generation will be one of the major trends in electricity networks in the long term. Solar will become the most important generation technology in the years to come [91]. The impact of the mentioned trends on the load curve may be better understood for further improved modeling in further research.

6. CONCLUSION

Electricity load forecasting is crucial for all stakeholders in electricity generation, distribution, transmission, markets and associated research and the respective development of long- and short-term strategies [1].

In this research, electricity consumption of 56 countries with real load data was analysed and a linear regression model in terms of oscillations of the daily, weekly and seasonal variations was developed. A key result had been that taking into account specific economic, technical and climate characteristics, such as high shares of marginal cost generation, air conditioning, impact of tourism and industrial consumption, local temperature and seasonal effects is necessary for improved modeling results.

The major contribution of this research is an electricity demand projection model based on UN targets for all countries globally from the present till the year 2100. The model further enables to distribute the selected annual electricity demand to all hours of a year, based on country specific data such as GDP/capita, geographic position, climate conditions and related parameters.

The obtained results demonstrate that the model performs well on the available data. It has been confirmed by R-square error values which vary between 0.968 – 0.998. In general, the results provide significant and insightful expectations for the long-range energy consumption.

The framework developed in this research provides an access to hourly resolution electricity demand in the possible future on a per country level and for this century, which can be very valuable for planning purposes. In addition, these results could have a significant impact and support in energy transition studies towards sustainability ahead, since it allows improved analysis in matching variable renewable energy generation and load demand for all countries in a structured and systematic manner.

7. REFERENCES

- [1] Weron R., 2006. Modeling and Forecasting Electricity Loads and Prices: A Statistical Approach. Wiley Finance, New York;
- [2] Filik Ü. B., Gerek Ö. N., Kurban M., 2011. A novel modeling approach for hourly forecasting of long-term electric energy demand, *Energy Conversion and Management*, 52 (1), 199-211;
- [3] Hyndman R. J., Fan S., 2010. Density forecasting for long-term peak electricity demand, *IEEE Transactions Power Syst.*, 25 (2), 1142–53;
- [4] Kyriakides E., Polycarpou M., 2007. Short term electric load forecasting: A tutorial, in: K. Chen, L. Wang (Eds.), *Trends in Neural Computation, Studies in Computational Intelligence*, Springer, 35, 391–418;
- [5] Hong T., Fan S., 2016. Probabilistic electric load forecasting: A tutorial review, *International Journal of Forecasting*, 32 (3), 914–938;
- [6] Hong T., Wilson J., Xie J., 2014. Long-term probabilistic load forecasting and normalization with hourly information, *IEEE Transactions on smart grid*, 5 (1), 456-462;
- [7] Hor C.-L., Watson S. J., Majithia S., 2005. Analyzing the Impact of Weather Variables on Monthly Electricity Demand, *IEEE Transactions on power systems*, 20 (4), 2078-2085;
- [8] Bianco V., Manca O., Nardini S., 2009. Electricity consumption forecasting in Italy using linear regression models, *Energy*, 34 (9), 1413–1421;
- [9] Mohamed Z., Bodger P., 2005. Forecasting electricity consumption in New Zealand using economic and demographic variables, *Energy*, 30 (10), 1833–1843;
- [10] Kankal M., Akpınar A., Kömürcü M. İ., Özşahin T.Ş., 2011. Modeling and forecasting of Turkey's energy consumption using socio-economic and demographic variables, *Appl. Energy*, 88, 1927–1939;
- [11] Yukseltan E., Yucekaya A., Bilge A. H., 2017. Forecasting electricity demand for Turkey: Modeling periodic variations and demand segregation, *Applied Energy*, 193, 287-296;
- [12] Trotter I. M., Bolkesjø T. F., Féres J. G., Hollanda L., 2016. Climate change and electricity demand in Brazil: A stochastic approach, *Energy*, 102, 596-604;

- [13] Mirasgedis S., Sarafidis Y., Georgopoulou E., Lalas D.P., Moschovits M., Karagiannis F., Papakonstantinou D., 2006. Models for mid-term electricity demand forecasting incorporating weather influences, *Energy*, 31, 208–227;
- [14] Amjady N., 2001. Short-Term Hourly Load Forecasting Using Time-Series Modeling with Peak Load Estimation Capability, *IEEE Trans. Power Syst.*, 16 (3), 498-505;
- [15] Clements A.E., Hurn A.S., Li Z., 2016. Forecasting day-ahead electricity load using a multiple equation time series approach, *European Journal of Operational Research*, 251 (2), 522–530;
- [16] Taylor J. W., Snyder R. D., 2012. Forecasting intraday time series with multiple seasonal cycles using parsimonious seasonal exponential smoothing, *Omega*, 40 (6), 748-757;
- [17] Günay M. E., 2016. Forecasting annual gross electricity demand by artificial neural networks using predicted values of socio-economic indicators and climatic conditions: Case of Turkey, *Energy Policy*, 90, 92–101;
- [18] Ekonomou L., 2010. Greek long-term energy consumption prediction using artificial neural networks, *Energy*, 35, 512–517;
- [19] Song K. B., Baek Y. S., Hong D. H., Jang G., 2005. Short-term load forecasting for the holidays using fuzzy linear regression method, *IEEE Trans. Power Syst.*, 20 (1), 96–101;
- [20] Tzafestas S., Tzafestas E., 2001. Computational intelligence techniques for short-term electric load forecasting, *J Intell Robo Syst*, 31, 7–68;
- [21] Torrini F.C., Souza R.C., Oliveira F.L.C., Pessanha J.F.M., 2016. Long-term electricity consumption forecast in Brazil: a fuzzy logic approach, *Soc. Econ. Plan. Sci*, 54, 18–27;
- [22] Kucukali S., Baris K., 2010. Turkey's short-term gross annual electricity demand forecast by fuzzy logic approach, *Energy Policy*, 38 (5), 2438-2445;
- [23] Afshin M., Sadeghian A., 2007. PCA-based least squares support vector machines in week-ahead load forecasting, *Industrial and Commercial Power System Technical Conference*, IEEE, 1–6;
- [24] Hahn H., Meyer-Nieberg S., Pickl S., 2009. Electric load forecasting methods: Tools for decision making, *European Journal of Operational Research*, 199 (3), 902–907;
- [25] Do L. P. C., Lin K.-H., Molnára P., 2016. Electricity consumption modelling: A case of Germany, *Economic Modelling*, 55, 92–101;

- [26] Pérez-Garcíaa J., Moral-Carcedob J., 2016. Analysis and long term forecasting of electricity demand through a decomposition model: A case study for Spain, *Energy*, 97, 127–143;
- [27] Mustapha M., Mustafa M. W., Khalid S. N., Abubakar I., Shareef H., 2015. Classification of electricity load forecasting based on the factors influencing the load consumption and methods used: An-overview, *2015 IEEE Conf. Energy Conversion CENCON*, 442-447;
- [28] Squalli J., 2007. Electricity consumption and economic growth: Bounds and causality analyses of OPEC mem, *Energy Economics*, 29, 1192–1205;
- [29] Shiu A., Lam P-L., 2004. Electricity consumption and economic growth in China, *Energy Policy*, 32, 47–54;
- [30] Ghosh S., 2002. Electricity consumption and economic growth in India, *Energy Policy*, 30, 125–129;
- [31] World Bank, 2017a. GDP per capita, PPP (constant 2011 international \$), Washington DC. Available: <http://data.worldbank.org/indicator/NY.GDP.PCAP.PP.KD>. [Accessed 02.06.2016];
- [32] Modis T., 2013. Long-term GDP forecasts and the prospects for growth, *Technological Forecasting and Social Change*, 80, 1557–1562;
- [33] [UN] – United Nations, 2015. Transforming our world: the 2030 Agenda for Sustainable Development, *Resolution adopted by the General Assembly*, New York;
- [34] [IEA] – International Energy Agency, 2015. Energy Balances of OECD Countries, Paris;
- [35] [IEA] – International Energy Agency, 2015. World Energy of non-OECD Countries, Paris;
- [36] Ferguson R., Wilkinson W., Hill R., 2000. Electricity consumption and economic development, *Energy Policy*, 28, 923-934;
- [37] [UN] – United Nations, 2015. Department of Economic and Social Affairs, Population Division, World Population Prospects, The 2015 Revision, New York. Available: <https://esa.un.org/unpd/wpp/DataQuery/>. [Accessed 02.06.2017];
- [38] Stackhouse P.W., Whitlock C.H., editors. 2008. Surface meteorology and solar energy (SSE) release 6.0, NASA SSE 6.0, earth science enterprise program. National Aeronautic and Space Administration (NASA), Langley. Available: <http://eosweb.larc.nasa.gov/sse/>. [Accessed 28.05.2015];
- [39] Stackhouse P.W., Whitlock C.H., editors. 2009. Surface meteorology and solar energy (SSE) release 6.0 Methodology, NASA SSE 6.0, earth science enterprise program, National

- Aeronautic and Space Administration (NASA), Langley. Available: <http://eosweb.larc.nasa.gov/sse/documents/SSE6Methodology.pdf>. [Accessed 28.05.2015];
- [40] Stetter D., 2012. Enhancement of the REMix energy system model: global renewable energy potentials optimized power plant siting and scenario validation. Dissertation, Faculty of Energy-, Process and Bio-Engineering, University of Stuttgart;
- [41] Koreneff G., Ruska M., Kiviluoma J., Shemeikka J., Lemström B., Alanen R., Koljonen T., 2009. Future development trends in electricity demand, VTT Tiedotteita – Research Notes 2470. 79 p, Espoo;
- [42] Knoema, 2017. World Data Atlas, Travel & Tourism Total Contribution to GDP - % share, McLean, VA. Available: <https://knoema.com/atlas/topics/Tourism/Travel-and-Tourism-Total-Contribution-to-GDP/Total-Contribution-to-GDP-percent-share>. [Accessed 02.06.2017];
- [43] World Bank, 2017b. Industry, value added (% of GDP), Washington DC. Available: <http://data.worldbank.org/indicator/NY.GDP.PCAP.PP.KD>. [Accessed 02.06.2016];
- [44] Bejtullahu N, 2014. Common Electricity Market Kosovo – Albania, *Workshop on the future role of energy storage in South Eastern Europe, Tirana*, October 21 – 22. Available: <https://setis.ec.europa.eu/system/files/Common%20Electricity%20Market%20Kosovo-Albania-USAID%20-%20BEJTULLAHU.pdf>. [Accessed 21.06.2017];
- [45] [ENTSO-E] – European Network of Transmission System Operators for Electricity, 2015. Data, Data Portal, Consumption, Brussels. Available: www.entsoe.eu/Pages/default.aspx. [Accessed 28.07.2016];
- [46] [CIGRE] – International council on large electric systems, 2015. The Electric Power System, Algeria Power System Paris. Available: www.cigre.org/var/cigre/storage/original/application/1ec62202f27aaa674c271ace096089f3.pdf. [Accessed 12.02.2017];
- [47] [SAPP] – Southern African Pool, 2016. Annual report 2016, Harare;
- [48] [Cammesa] – Compañía Administradora del Mercado Mayorista Eléctrico, 2016. Diego Margulis, Private communication, Buenos Aires, October 10;
- [49] [AEMO] – Australian Energy Market Operator, 2016. National Electricity Market, Melbourne. Available: www.aemo.com.au/Electricity/National-Electricity-Market-NEM/Data-dashboard#aggregated-data. [Accessed 28.07.2016];

- [50] Blechinger, P. (ed.), 2015. Barriers and solutions to implementing renewable energies on Caribbean islands in respect of technical, economic, political, and social conditions, PhD thesis TU Berlin, Shaker Verlag, Berlin;
- [51] [BPC] – Botswana Power Corporation 2015. 2015 Annual Report, Gaborone Available: www.bpc.bw/about-us/Annual%20Reports/BPC%20Annual%20Report%202015.pdf. [Accessed 25.06.2017];
- [52] [ANEEL] – Agência Nacional de Energia Elétrica, 2016. Private communication, Brasília, October 7;
- [53] [ADB] – Asian Development Bank, Nam K.-Y., Cham M. R., Halili P. R. 2015. Power Sector Development in Myanmar, *ADB Economics Working Paper Series*, 460, Mandaluyong;
- [54] [ICA] – The Infrastructure Consortium for Africa 2011. Regional Power Status in African Power Pools Report, Cote d'Ivoire;
- [55] [ADB] – Asian Development Bank, 2012. Greater Mekong Subregion Power Trade and Interconnection, 2 Decades of Cooperation, Mandaluyong. Available: www.adb.org/sites/default/files/publication/29982/gms-power-trade-interconnection.pdf. [Accessed 22.06.2017];
- [56] [IESO] – The Independent Electricity System Operator, 2016. Private communication, Toronto. Available: www.ieso.ca/. [Accessed 28.07.2016];
- [57] [SaskPower] – Saskatchewan Power Corporation, 2016. Private communication, Saskatchewan. Available: www.saskpower.com/. [Accessed 28.07.2016];
- [58] [CDEC-SING] – Coordinador Eléctrico Nacional, 2016. Private communication, Santiago. Available: www.coordinadorelectrico.cl/. [Accessed 22.06.2017];
- [59] [IRENA] – International Renewable Energy Agency, 2014. Renewable Energy Prospects: China, Abu Dhabi. Available: https://irena.org/remap/IRENA_REmap_China_report_2014.pdf. [Accessed 22.06.2017];
- [60] Bedoya Díaz H.A., 2013. Private communication;
- [61] Arab Republic of Egypt, Ministry of Electricity and Renewable Energy, 2013. Annual report 2014-2015., Cairo. Available: www.moee.gov.eg/english_new/EEHC_Rep/2014-2015en.pdf. [Accessed 22.06.2017];

- [62] Ashenafi A. Demissie, Solomon A.A., 2016. Power system sensitivity to extreme hydrological conditions as studied using an integrated reservoir and power system dispatch model, the case of Ethiopia, *Applied Energy*, 182, pp. 442–463;
- [63] [GRIDCo] – Ghana grid company limited, 2011. 2014 Electricity supply plan, Tema. Available: www.gridcogh.com/media/photos/forms/supplyplan/2014_Electricity_Supply_Plan.pdf. [Accessed 22.06.2017];
- [64] [CEA] – Central Electricity Authority, 2016. Load Generation Balance Report 2016-17, New Delhi. Available: www.cea.nic.in/reports/annual/lgbr/lgbr-2016.pdf. [Accessed 22.06.2017];
- [65] [IAEA-CNPP] – International Atomic Energy Agency, Country Nuclear Power Profiles, 2016, Indonesia, Vienna. Available: <https://cnpp.iaea.org/countryprofiles/Indonesia/Indonesia.htm>. [Accessed 22.06.2017];
- [66] [IGMC] - Iran Grid Management Company, 2016. Definitive Report 1394 [in Persian], Tehran. Available: www.igmc.ir/Documents-Management?EntryId=305927. [Accessed 19.04.2016];
- [67] Without author, 2015. Load curve for Israel, private communication;
- [68] [METI] – Ministry of Economy Energy and Industry, 2012. Load curve for Japanese grid areas, Tokyo. Available: www.meti.go.jp/setsuden/performance.html. [Accessed 21.06.2016];
- [69] Baraza M., 2015. Private communication;
- [70] [KPX] – Korea Power Exchange, 2015. Private communication, Jeollanam-do. Available: www.kpx.or.kr/. [Accessed 21.06.2017];
- [71] Suruhanjaya Tenaga (Energy Commission), 2015. National Energy Balance 2014, Putrajaya. Available: www.st.gov.my/index.php/en/. [Accessed 21.06.2017];
- [72] [SENER] – Secretaria De Energia, 2010. Private communication, Mexico. Available: <http://sie.energia.gob.mx/bdiController.do?action=temas&fromCuadros=true>. [Accessed 18.05.2016];
- [73] Giuliano S., Puppe M., Schenk H., Hirsch T., Moser M., Fichter T., Kern J., Trieb F., Brakemeier D., Kretschmann J., Haller U., Klingler R., Engelhard M., Hurler S., Weigand

- A., Breyer Ch., Afanasyeva S., 2016. Techno-Economic Analysis and Comparison of CSP and Hybrid PV-Battery Power Plants, SolarPACES, Abu Dhabi, October 11-14;
- [74] [EMI] – Electricity Authority, 2016. Grid demand trend, Wellington. Available: www.emi.ea.govt.nz. [Accessed 20.09.2016];
- [75] [NTDC] – National Transmission And Despatch Company Limited, 2016. Power System Statistics 2013-2014, Lahore. Available: www.ppib.gov.pk/Power%20System%20Statistics%202013-14.pdf. [Accessed 22.06.2017];
- [76] [WESM] – Wholesale Electricity Spot Market, 2012. Downloads, Annual Market Assessment Report - 2015, Pasig. Available: www.wesm.ph/. [Accessed 22.06.2017];
- [77] [UES] – System Operator of the Unified Energy System, 2015. Generation and Consumption (hour) [in Russian], Moscow. Available: www.so-cdu.ru/. [Accessed 22.12.2015];
- [78] [ECRA] – Electricity and Cogeneration Regulatory Authority, 2016. Private communication, Arriyadh. Available: www.ecra.gov.sa/en-us/dataandstatistics/pages/DataAndStatistics.aspx. [Accessed 22.06.2017];
- [79] [CEB] – Ceylon Electricity Board, 2015. Long Term Generation Expansion Plan 2015-2034, Colombo. Available: <http://pucsl.gov.lk/sinhala/wp-content/uploads/2015/09/Long-Term-Generation-Plan-2015-2034-PUCSL.pdf>. [Accessed 22.06.2017];
- [80] [EMA] – Energy Market Authority of Singapore, 2017. Statistics, Electricity, Demand, Bukit Merah. Available: www.ema.gov.sg/index.aspx. [Accessed 22.06.2017];
- [81] [EPPO] – Energy Policy and Planning Office, Ministry of Energy, 2016. Energy Statistics, Electricity, Bangkok. Available: www.eppo.go.th/index.php/en/. [Accessed 21.06.2017];
- [82] Dii, 2013. Common research on future energy options for Tunisia, Munich;
- [83] [TurkStat] – Turkish Statistical Institute, 2016. Private communication, Ankara. Available: www.turkstat.gov.tr/Start.do. [Accessed 21.06.2017];
- [84] [Statista] – The Statistical Portal, 2016. Industries, Energy & Environmental Services, Electricity, U.S. electric noncoincident peak load 1990-2013, New York. Available: www.statista.com/. [Accessed 21.06.2017];
- [85] Hà N.H., 2013. EVN Smart Grid Plan, *PEP-Fachveranstaltung*, Frankfurt, November 14. Available: www.giz.de/fachexpertise/downloads/2013-en-pep-fachveranstaltung-smart-grids-nguyen-hai-ha.pdf. [Accessed 21.06.2017];

- [86] [Statista] – The Statistical Portal, 2015. Industries, Energy & Environmental Services, Electricity, U.S. electric noncoincident peak load 1990-2013, New York. Available: www.statista.com/. [Accessed 21.06.2017];
- [87] [EIA]-The U.S. Energy Information Administration, 2015. International Energy Statistics, Statistics, Washington, DC. Available: www.eia.gov/ [Accessed 21.06.2017];
- [88] [IEA]-International Energy Agency, 2015a. Key World Energy Statistics 2015, Statistics, Paris;
- [89] [IEA]-International Energy Agency, 2015b. Key World Energy Statistics 2011, Statistics, Paris;
- [90] [IEA]-International Energy Agency, 2015c. Key World Energy Statistics 2012, Statistics, Paris;
- [91] Breyer Ch., Bogdanov D., Gulagi A., Aghahosseini A., Barbosa L.S.N.S., Koskinen O., Barasa M., Caldera U., Afanasyeva S., Child M., Farfan J., Vainikka P., 2017. On the Role of Solar Photovoltaics in Global Energy Transition Scenarios, *Progress in Photovoltaics: Research and Applications*, 25, 727-745;

8. APPENDIX

Table A1. References for available load data.

Country	Year	Type of data	Author/ Authority	Reference
Albania	2012	peak	Naim Bejtullahu	[44]
Algeria	2014	peak	Cigre	[46]
Angola	2015	peak	SAPP	[47]
Argentina	2015	full load curve	Cammesa	[48]
Australia	2015	full load curve	AEMO	[49]
Austria	2015	full load curve	ENTSO-E	[45]
Barbados	2010	full load curve	Blechinger, P.	[50]
Belgium	2015	full load curve	ENTSO-E	[45]
Bosnia and Herzegovina	2015	full load curve	ENTSO-E	[45]
Botswana	2015	peak	BPC	[51]
Brazil	2015	full load curve	ANEEL	[52]
Bulgaria	2015	full load curve	ENTSO-E	[45]
Myanmar former Burma	2013	peak	ADB	[53]
Burundi	2009	peak	ICA	[54]
Cambodia	2015	peak	ADB	[55]
Cameroon	2009	peak	ICA	[54]
Canada	2015	full load curve	IESO, SaskPower	[56], [57]
Central African Republic	2009	peak	ICA	[54]
Chad	2009	peak	ICA	[54]
Chile	2015	full load curve	CDEC-SING	[58]
China	2013	peak	IRENA	[59]
Colombia	2010	full load curve	Bedoya Díaz H.A.	[60]
Croatia	2015	full load curve	ENTSO-E	[45]
Cyprus	2015	full load curve	ENTSO-E	[45]
Czech Republic	2015	full load curve	ENTSO-E	[45]
Denmark	2010	full load curve	ENTSO-E	[45]
Djibouti	2010	peak	ICA	[54]
Egypt	2013	peak	Ministry of Electricity and Renewable Energy	[61]
Estonia	2015	full load curve	ENTSO-E	[45]

Ethiopia	2013	full load curve	Ashenafi A. Demissie, A.A. Solomon	[62]
Finland	2015	full load curve	ENTSO-E	[45]
France	2015	full load curve	ENTSO-E	[45]
Gabon	2009	peak	ICA	[54]
Germany	2015	full load curve	ENTSO-E	[45]
Ghana	2014	peak	GRIDCo	[63]
Greece	2015	full load curve	ENTSO-E	[45]
Hungary	2015	full load curve	ENTSO-E	[45]
Iceland	2015	full load curve	ENTSO-E	[45]
India	2015	full load curve	CEA	[64]
Indonesia	2013	peak	IAEA-CNPP	[65]
Iran	2015	full load curve	IGMC	[66]
Ireland	2015	full load curve	ENTSO-E	[45]
Israel	2013	full load curve	without author	[67]
Italy	2015	full load curve	ENTSO-E	[45]
Japan	2010	full load curve	MIET	[68]
Kenya	2010	full load curve	Baraza M.	[69]
Korea Republic	2015	full load curve	KPX	[70]
Latvia	2015	full load curve	ENTSO-E	[45]
Lesotho	2015	peak	SAPP	[47]
Libya	2009	peak	ICA	[54]
Lithuania	2015	full load curve	ENTSO-E	[45]
Luxemburg	2010	full load curve	ENTSO-E	[45]
Macedonia Republic	2015	full load curve	ENTSO-E	[45]
Malawi	2015	peak	SAPP	[47]
Malaysia	2014	peak	Suruhanjaya Tenaga	[71]
Mexico	2011	full load curve	SENER	[72]
Morocco	2010	full load curve	Giuliano S.	[73]
Namibia	2015	peak	SAPP	[47]
Netherlands	2015	full load curve	ENTSO-E	[45]
New Zealand	2015	full load curve	EMI	[74]
Nigeria	2010	peak	ICA	[54]
Norway	2015	full load curve	ENTSO-E	[45]
Pakistan	2013	peak	NTDC	[75]
Philippines	2015	peak	WESM	[76]

Poland	2015	full load curve	ENTSO-E	[45]
Portugal	2015	full load curve	ENTSO-E	[45]
Romania	2015	full load curve	ENTSO-E	[45]
Russian Federation	2014	full load curve	UES	[77]
Rwanda	2010	peak	ICA	[54]
Saudi Arabia	2013	full load curve	ECRA	[78]
Singapore	2015	full load curve	EMA	[80]
Slovakia	2015	full load curve	ENTSO-E	[45]
Slovenia	2015	full load curve	ENTSO-E	[45]
South Africa	2015	peak	SAPP	[47]
Spain	2015	full load curve	ENTSO-E	[45]
Sri Lanka	2013	full load curve	CEB	[79]
St. Vincent and the Grenadines	2010	full load curve	Blechinger, P.	[50]
Sudan	2010	peak	ICA	[54]
Swaziland	2015	peak	SAPP	[47]
Sweden	2015	full load curve	ENTSO-E	[45]
Switzerland	2015	full load curve	ENTSO-E	[45]
Tanzania.	2015	peak	SAPP	[47]
Thailand	2015	peak	EPPO	[81]
Tunisia	2010	full load curve	Dii	[82]
Turkey	2015	full load curve	TurkStat	[83]
Uganda	2010	peak	ICA	[54]
United Kingdom	2015	full load curve	ENTSO-E	[45]
United States	2013	peak	Statista	[84], [86]
Vietnam	2013	peak	Hà N.H.	[85]
Serbia	2015	full load curve	ENTSO-E	[45]
Zambia	2015	peak	SAPP	[47]
Zimbabwe	2015	peak	SAPP	[47]
Montenegro	2015	full load curve	ENTSO-E	[45]

Table A2. R-squared error

Countries	Year	Error
Argentina	2015	0.98
Australia	2015	0.99
Austria	2015	0.99
Barbados	2010	0.99
Belgium	2015	0.99
Bosnia-Herzegovina	2015	0.99
Brazil	2015	0.99
Bulgaria	2015	0.99
Canada	2015	0.99
Chile	2015	0.99
Colombia	2010	0.99
Croatia	2015	0.99
Cyprus	2015	0.97
Czech Republic	2015	0.99
Denmark	2010	0.99
Estonia	2015	0.99
Ethiopia	2013	0.98
Finland	2015	0.99
France	2015	0.98
Germany	2015	0.99
Greece	2015	0.99
Hungary	2015	0.99
Iceland	2015	1
Iran	2015	0.99
Ireland	2015	0.99
Israel	2013	0.97
Italy	2015	0.98
Japan	2010	0.99
Kenya	2010	0.98
Korea Republic	2015	0.99
Latvia	2015	0.99
Lithuania	2015	0.99
Luxembourg	2010	0.98
Macedonia	2015	0.98
Mexico	2011	0.99
Morocco	2010	0.99
Netherlands	2015	0.99
New Zealand	2015	0.99
Norway	2015	0.99

Poland	2015	0.99
Portugal	2015	0.98
Romania	2015	0.99
Russia	2014	1
Saudi Arabia	2013	0.98
Serbia	2015	0.98
Singapore	2015	0.99
Slovakia	2015	0.99
Slovenia	2015	0.99
Spain	2015	0.99
Sri Lanka	2013	0.98
St. Vincent and the Grenadines	2010	0.97
Sweden	2015	0.99
Switzerland	2015	0.99
Tunisia	2010	0.97
Turkey	2015	0.98
United Kingdom	2015	0.98

Table A3. Peal peak load, modelled peak load and deviation

Countries	Year	Real Peak [MW]	Model Peak [MW]	Deviation [%]
Albania	2012	1485	1210	-18.5
Algeria	2014	11188	11240	0.5
Angola	2015	1599	1470	-8.1
Argentina	2015	22051	18030	-18.2
Australia	2015	34545	30340	-12.2
Austria	2015	11386	11020	-3.2
Barbados	2010	163	156	-4.3
Belgium	2015	13129	13010	-0.9
Bosnia-Herzegovina	2015	2105	2100	-0.2
Botswana	2015	711	597	-16.0
Brazil	2015	91294	87120	-4.6
Bulgaria	2015	7100	6380	-10.1
Myanmar	2013	2001	1790	-10.5
Burundi	2009	42	43	2.4
Cambodia	2015	1008	855	-15.2
Cameroon	2009	708	763.41	7.8
Canada	2015	53900	52110	-3.3
Central African Republic	2009	55	29	-47.3
Chad	2009	24	31	29.2
Chile	2015	9094	9109	0.2
China	2013	654000	604010	-7.6
Colombia	2010	9978	8420	-15.6
Croatia	2015	2950	2680	-9.2
Cyprus	2015	954	689	-27.8
Czech Republic	2015	10001	9829	-1.7
Denmark	2010	5844	5550	-5.0
Djibouti	2010	75	65	-13.3
Egypt	2013	26140	25030	-4.2
Estonia	2015	1394	1320	-5.3
Ethiopia	2013	1418	1340	-5.5
Finland	2015	13584	12196	-10.2
France	2015	91611	73960	-19.3
Gabon	2009	197	216	9.6
Germany	2015	77496	77105	-0.5
Ghana	2014	2180	2200	0.9
Greece	2015	9813	7954	-18.9
Hungary	2015	6106	6202	1.6
Iceland	2015	2327	2477	6.4

India	2015	148166	152790	3.1
Indonesia	2013	30834	29020	-5.9
Iran	2015	46155	53166	15.2
Ireland	2015	4662	4078	-12.5
Israel	2013	11394	8469	-25.7
Italy	2015	59648	47904	-19.7
Japan	2010	177757	165448	-6.9
Kenya	2010	1139	983	-13.7
Korea Republic	2015	74200	69723	-6.0
Latvia	2015	1225	1188	-3.0
Libya	2009	5282	4300	-18.6
Lithuania	2015	1748	1688	-3.4
Luxembourg	2010	1107	1041	-6.0
Macedonia	2015	1439	1319	-8.3
Malawi	2015	326	468.24	43.6
Malaysia	2014	16901	16630	-1.6
Mexico	2011	51606	47670	-7.6
Morocco	2010	4745	4694	-1.1
Namibia	2015	629	667	6.0
Netherlands	2015	17761	17674	-0.5
New Zealand	2015	3228	2987	-7.5
Nigeria	2010	3804	3530	-7.2
Norway	2015	22530	19943	-11.5
Pakistan	2013	18827	14500	-23.0
Philippines	2015	10337	11000	6.4
Poland	2015	23069	23373	1.3
Portugal	2015	8618	7525	-12.7
Romania	2015	8488	8350	-1.6
Russia	2014	154699	151410	-2.1
Rwanda	2010	53	58	9.4
Saudi Arabia	2013	53798	53786	0.0
Serbia	2015	6879	6578	-4.4
Singapore	2015	6960	7230	3.9
Slovakia	2015	4145	4396	6.1
Slovenia	2015	2086	2079	-0.3
South Africa	2015	36170	33340	-7.8
Spain	2015	40324	38345	-4.9
Sri Lanka	2013	2164	1743	-19.5
St. Vincent and the Grenadines	2010	21	20	-4.8
Sudan	2010	1357	1200	-11.6
Swaziland	2015	221	249	12.7
Sweden	2015	23395	23199	-0.8

Switzerland	2015	10155	9763	-3.9
Tanzania	2015	935	1800	92.5
Thailand	2015	27300	26620	-2.5
Tunisia	2010	2992	2527	-15.5
Turkey	2015	42482	37077	-12.7
Uganda	2010	596	408	-31.5
United Kingdom	2015	52427	43802	-16.5
United States	2013	758953	686940	-9.5
Vietnam	2013	19772	17440	-11.8
Zambia	2015	1987	2200	10.7
Zimbabwe	2015	1671	1560	-6.6

Table A4. Annual electricity demand (TWh) for all countries in the world for the years 2015, 2030, 2050, 2070 and 2090, based on the assumptions in this research.

Countries	2015	2030	2050	2070	2090
Afghanistan	4.7	31.2	311.9	878.2	1053.5
Albania	8.1	16.4	30.8	37.1	34.3
Algeria	63.1	227.8	672.2	980.0	1091.2
Angola	9.4	113.3	532.2	1321.3	2162.8
Antigua and Barbuda	0.3	0.7	1.5	1.9	2.0
Argentina	132.1	375.9	757.8	970.4	1050.1
Armenia	6.3	19.3	36.9	38.5	34.5
Australia	215.4	351.4	540.0	663.4	738.2
Austria	69.6	99.5	134.0	147.5	150.0
Azerbaijan	24.3	60.9	122.4	162.0	174.0
Bahamas. The	1.8	2.7	6.2	8.4	8.9
Bahrain	23.4	26.2	28.0	29.2	29.6
Bangladesh	62.3	276.1	1177.3	2486.3	3056.9
Barbados	1.1	1.4	2.7	4.1	4.6
Belarus	37.3	62.7	97.1	116.6	124.4
Belgium	85.2	111.4	163.4	208.4	232.0
Belize	0.6	1.3	4.2	9.1	11.7
Benin	1.7	11.2	122.7	409.8	594.4
Bermuda	0.6	0.7	0.9	0.8	0.8
Bhutan	1.8	3.6	8.1	12.7	14.4
Bolivia	9.1	29.7	110.5	236.3	313.0
Bosnia-Herzegovina	12.4	17.8	32.3	38.8	36.5
Botswana	3.6	11.7	29.8	50.7	63.7
Brazil	581.0	1169.3	2553.6	3560.5	3709.5
Brunei	3.7	5.7	8.3	9.3	9.0
Bulgaria	38.6	50.8	67.1	67.7	64.1
Burundi	0.4	2.8	114.4	635.6	998.4
Cambodia	5.0	22.8	114.2	296.9	412.7
Cameroon	7.7	31.1	275.3	913.3	1359.1
Canada	342.4	542.8	759.7	838.2	880.9
Cape Verde	0.4	2.0	6.3	10.5	12.2
Central African Republic	0.0	4.2	55.8	155.3	212.8
Chad	2.2	23.4	193.1	637.5	1082.1
Chile	69.3	127.8	222.7	310.0	351.6
China	4900.8	10469.4	16769.8	18985.5	18644.7
Colombia	82.0	205.6	491.4	753.5	829.8
Comoros	0.2	2.8	15.5	29.3	38.5

Congo Democratic Republic	20.0	149.0	1331.5	3912.8	6210.6
Congo Republic	1.9	14.3	100.0	239.8	353.6
Costa Rica	11.0	26.9	58.7	84.3	91.2
Croatia	17.2	27.4	41.7	48.6	48.5
Cuba	21.0	62.1	130.7	144.9	135.4
Cyprus	4.4	10.1	19.1	23.7	24.8
Czech Republic	63.5	93.4	131.1	150.3	157.4
Denmark	37.4	53.2	78.7	102.4	118.2
Djibouti	0.4	1.4	6.3	15.0	19.7
Dominica	0.1	0.3	0.8	1.0	1.0
Dominican Republic	19.6	51.0	116.1	182.7	215.1
Ecuador	24.9	89.0	280.7	404.4	442.5
Egypt	162.4	681.2	2042.8	2944.7	3482.6
El Salvador	6.7	31.9	84.5	96.9	87.5
Equatorial Guinea	0.6	7.9	22.2	38.5	50.1
Eritrea	0.8	17.5	131.7	216.6	266.8
Estonia	7.9	8.8	11.3	14.4	16.1
Ethiopia	14.6	180.9	1417.3	3277.4	4233.8
Fiji	1.0	2.3	6.8	12.0	13.1
Finland	82.5	89.8	100.6	102.7	105.3
France	471.3	667.7	980.4	1207.6	1335.7
Gabon	3.2	8.8	29.1	58.3	76.3
Gambia, The	0.3	2.1	16.9	71.0	137.8
Georgia	9.0	17.5	34.6	44.5	45.4
Germany	505.3	757.9	1052.1	1161.9	1153.6
Ghana	13.2	101.4	543.3	986.5	1246.2
Greece	51.3	62.8	92.9	122.9	133.9
Grenada	0.2	0.4	1.0	1.4	1.4
Guatemala	11.3	42.4	214.9	480.6	608.0
Guinea	1.3	10.9	150.7	530.4	801.6
Guinea - Bissau	0.5	6.5	37.0	70.2	92.0
Guyana	0.7	2.4	7.3	11.2	11.3
Haiti	1.2	22.9	151.7	234.3	248.6
Honduras	6.4	15.4	52.4	128.8	183.8
Hong Kong	51.3	86.0	119.9	135.0	140.0
Hungary	40.8	77.0	108.1	119.5	119.6
Iceland	18.3	14.4	9.6	6.8	7.0
India	1068.9	4713.7	15448.4	25748.9	29767.4
Indonesia	267.3	1110.2	3098.2	4849.0	5584.3
Iran	269.7	461.9	899.8	1237.9	1290.4
Iraq	51.4	215.5	771.0	1683.0	2591.3

Ireland	26.6	52.9	83.9	102.5	112.4
Israel	62.4	96.9	157.6	229.9	292.1
Italy	314.3	383.9	534.1	731.1	867.1
Ivory Coast	7.0	25.3	240.4	981.2	1598.1
Jamaica	3.4	6.0	18.0	33.5	33.4
Japan	994.5	961.5	1002.7	1237.6	1454.6
Jordan	17.0	33.4	84.2	165.1	235.7
Kazakhstan	100.3	169.6	280.9	376.3	435.9
Kenya	12.8	103.2	1020.3	2038.4	2645.8
Kiribati	0.0	0.1	1.0	3.0	4.1
Korea Democratic Peoples Republic	15.6	26.4	168.5	376.1	444.1
Korea Republic	498.9	584.5	651.6	688.6	698.4
Kuwait	57.5	79.4	98.4	108.2	114.6
Kyrgyzstan	10.4	16.0	47.0	109.9	154.5
Laos	4.6	24.1	89.0	158.5	186.8
Latvia	7.1	10.3	15.9	20.8	22.9
Lebanon	17.4	28.3	59.4	84.3	87.7
Lesotho	0.2	2.2	11.9	35.8	58.0
Liberia	0.4	4.2	51.0	168.6	260.8
Libya	13.1	54.7	110.7	139.4	148.6
Lithuania	10.9	15.3	22.8	31.0	35.5
Luxembourg	8.0	10.8	13.8	16.1	17.7
Macedonia	7.8	11.7	22.6	27.8	27.6
Madagascar	2.4	12.2	164.0	957.7	1680.7
Malawi	2.6	11.6	213.0	880.7	1399.1
Malaysia	117.7	273.8	520.3	686.4	735.1
Maldives	0.4	1.5	4.2	7.0	7.9
Mali	1.8	18.3	253.5	938.1	1492.5
Malta	2.2	3.7	5.3	6.3	6.4
Mauritania	1.5	8.1	60.9	155.2	217.2
Mauritius	3.2	6.7	11.9	16.0	17.3
Mexico	400.6	734.5	1612.1	2471.1	2723.4
Moldova	6.0	11.9	27.0	36.2	35.1
Mongolia	5.6	17.2	43.0	66.3	78.3
Montenegro	3.4	4.1	5.7	7.4	8.0
Morocco	39.2	126.4	391.6	650.2	739.8
Mozambique	12.9	47.7	377.7	1219.6	2023.0
Myanmar former Burma	18.3	149.1	626.7	952.4	1017.1
Namibia	4.0	13.0	44.1	79.5	99.3
Nepal	5.6	35.0	215.2	488.5	557.7
Netherlands	113.3	167.5	235.4	281.7	305.0

New Caledonia	2.8	3.6	5.2	6.5	7.4
New Zealand	19.7	37.9	64.7	90.1	106.1
Nicaragua	4.3	12.2	44.6	98.7	125.4
Niger	4.1	43.2	503.5	1767.0	3171.8
Nigeria	80.6	810.8	4192.5	8639.1	12231.6
Norway	128.7	127.7	121.5	122.3	135.7
Oman	25.7	51.7	89.1	106.5	106.1
Pakistan	109.6	439.0	2238.8	4999.1	6367.9
Panama	9.6	28.7	63.9	93.4	106.9
Papua New Guinea	3.9	14.0	95.3	233.0	307.3
Paraguay	11.1	30.5	101.0	148.9	158.4
Peru	48.6	194.3	507.7	704.6	757.2
Philippines	68.2	349.5	1344.8	2443.8	2960.4
Poland	150.0	298.7	428.5	456.7	421.5
Portugal	48.9	62.2	90.1	117.8	132.6
Puerto Rico	19.6	28.9	41.3	46.3	42.8
Qatar	37.1	48.5	58.4	62.0	59.0
Romania	52.3	131.9	206.7	212.0	201.3
Russia	990.9	1107.9	1465.9	1850.0	2080.7
Rwanda	1.6	38.4	266.6	408.4	460.8
Sao Tome and Principe	0.1	0.3	2.8	7.0	9.1
Saudi Arabia	301.1	426.7	615.3	766.2	849.5
Senegal	3.7	14.4	138.6	655.3	1172.8
Serbia	39.5	46.1	69.7	92.4	98.0
Seychelles	0.3	0.7	1.2	1.5	1.5
Sierra Leone	0.9	11.8	96.3	205.8	254.6
Singapore	50.1	85.9	110.9	114.0	105.6
Slovakia	28.2	35.1	48.2	61.5	66.9
Slovenia	13.6	19.4	25.8	28.9	30.4
Solomon Island	0.1	0.6	5.5	16.9	23.1
Somalia	0.8	18.1	175.2	536.2	908.0
South Africa	233.1	321.7	675.9	1046.7	1181.7
Spain	248.5	367.5	530.5	633.9	684.3
Sri Lanka	18.0	88.9	213.3	283.1	283.4
St. Vincent and the Grenadines	0.2	0.5	1.3	1.6	1.5
Sudan	15.6	96.8	509.3	1333.7	2063.0
Swaziland	1.5	3.6	13.0	28.3	36.3
Sweden	135.9	168.3	209.2	230.7	252.4
Switzerland	62.1	97.1	143.2	176.5	195.5
Syria	28.3	100.5	321.5	561.3	674.9
Tajikistan	14.7	44.5	180.7	273.5	323.1

Tanzania. United Republic of	9.9	102.1	996.7	2970.6	4725.3
Thailand	174.8	468.5	837.0	873.9	798.8
Togo	2.9	27.7	163.2	328.6	455.5
Trinidad and Tobago	9.2	13.5	17.2	18.5	18.3
Tunisia	18.4	54.2	137.6	203.3	225.4
Turkey	263.5	545.9	1081.9	1487.2	1605.3
Turkmenistan	15.8	31.2	62.0	90.5	101.6
Uganda	5.5	113.2	1091.1	2355.6	3316.4
Ukraine	161.8	228.8	399.7	474.4	484.9
United Arab Emirates	103.0	149.7	208.3	238.0	242.1
United Kingdom	282.2	714.7	1215.3	1406.4	1467.6
United States	4850.1	6150.0	7115.0	7482.5	7952.0
Uruguay	11.8	24.7	45.2	57.3	59.8
Uzbekistan	54.3	148.5	414.2	570.1	593.3
Vanuatu	0.1	0.3	3.8	9.2	11.6
Venezuela	98.9	190.0	496.6	707.9	762.0
Vietnam	130.2	451.4	1266.0	1766.3	1897.1
Yemen	6.9	33.4	241.0	704.7	909.1
Zambia	12.9	51.2	347.7	978.5	1614.1
Zimbabwe	8.8	39.0	310.5	579.2	702.8
Region					
Africa	510.5	2641.8	17052.1	42876.2	63792.5
Eurasia	1263.4	1678.1	2741.7	3631.8	4067.3
Europe	3631.8	5681.1	8602.4	10338.1	10968.8
India South Asian Association for Regional Cooperation	1271.3	5589.1	19617.3	34903.7	41109.2
Middle East and North Africa	1297.2	2896.4	6987.0	10893.9	13169.8
North America	5672.2	7619.9	9978.5	11474.3	12273.7
Northeast Asia	6466.8	12145.1	18755.5	21489.1	21460.2
South America	1119.3	2598.0	6097.8	8856.9	9659.6
Southeast Asia	1083.0	3351.3	8738.9	13187.0	14920.7
Continent					
Africa	809.9	3792.9	20418.9	47809.7	69497.5
Americas	6791.5	10217.9	16076.2	20331.1	21933.3
Asia-Pacific	10041.9	23308.2	51851.0	77138.2	86754.5
Europe	4672.2	6881.6	10225.0	12371.8	13236.5
World	22315.5	44200.7	98571.1	157650.9	191421.8

Figures A5. Synthetic load curve diagrams for all countries, regions and the world for the year 2030 based on the model of this research.

